Electronic Supplementary Material (ESI) for Molecular BioSystems

Development of Diacyltetrol Lipids as Activator for the C1 Domain of Protein Kinase C

Narsimha Mamidi, Sukhamoy Gorai, Rakesh Mukherjee and Debasis Manna*

Table of Content

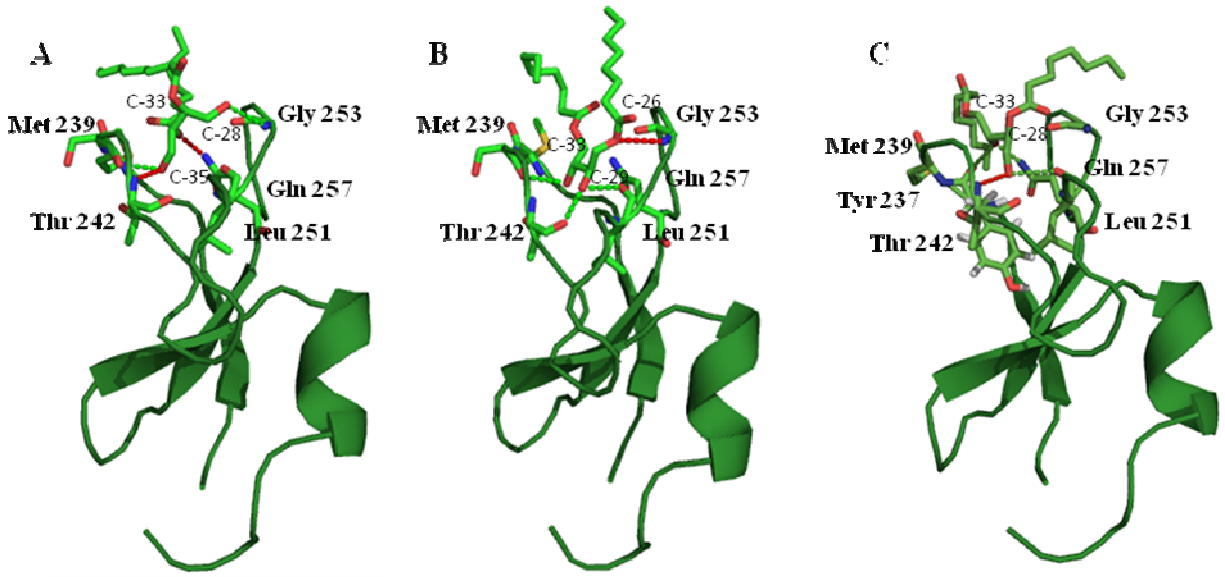

Figure S1: Structures of ligand bound PKCδ C1b subdomain. (**A**-**C**) modeled structure of short chain diacyltertol derivative (**1b, 2b, 3b**) docked into PKCδ C1b.The modeled structures are generated using the Molegro Virtual Docker, version 4.3.0. The oxygen atoms and nitrogen atoms are shown in red and blue, respectively. The dotted line indicates possible hydrogen bonds.

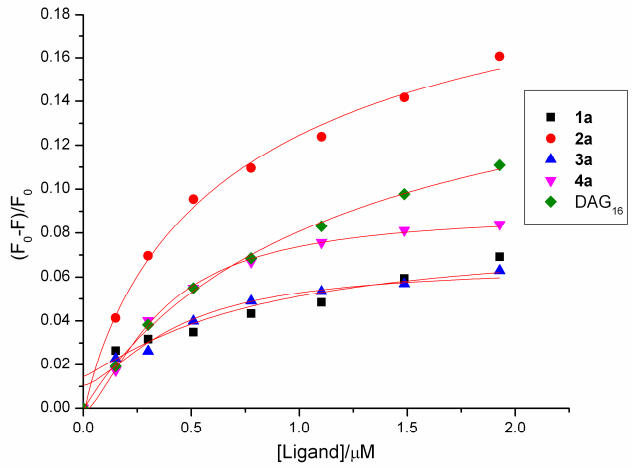

Figure S2: Binding of liposome containing ligands with PKCδ C1b. Representative plot of fluorescence intensity of PKCδ C1b (500 nM) in buffer (50 mM Tris, 150 mM NaCl, 50 μM ZnSO4, pH 7.4) in presence of varying concentration of liposome containing **1a** (■), **2a** (●), **3a** (▲), **4a** (▼) and DAG_{16} (♦), where F and F_0 are fluorescence intensity in the presence and absence of the ligand, respectively. Solid lines indicate the fit using Hill equation.

Competitive binding assay

In this approach, soluble DAT (**4b**) was employed as a competitive ligand. The protein (500 nM) was added to PC/PE/PS/DAG_{16}/NBD-PE (50:20:20:5:5) liposomes prepared by extrusion method and the emission spectra of NBD were monitored with the excitation wavelength of 280 nm. The compound **4b** was added (0 – 20 μM) and the decrease in NBD fluorescence intensity was monitored at 524 nm.

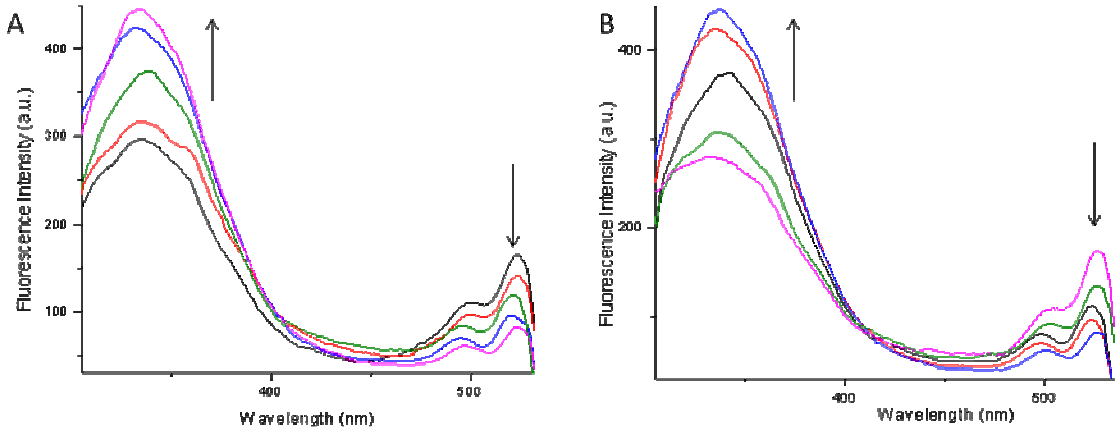

Figure S3: Representative plot of competitive binding of DAT **4b** to PKCδ C1b (A) and PKCθ C1b (B) bound DAG containing liposomes. The curve represents the emission spectrum (λ_{ex} = 280 nm) of a sample in which the protein (0.5 μM) was added to PC/PE/PS/DAG_{16}/NBD-PE (50:20:20:5:5) liposomes. The decrease in FRET efficiency between Trp residues (of PKCδ and PKC θ C1b sundomains) and NBD, caused by the displacement of protein from labeled liposmes, is demonstrated by the increase in Trp fluorescence (340 nm) and the concomitant decrease in NBD emission (524 nm).

Table S1: Docking score values obtained from the docking of DATs (with short chain length) and diC_8 into the PKCδ C1b subdomains using Molegro Virtual Docker, version 4.3.0.

Compound	Mol Dock score	Rerank score
diC8	-93.4027	-68.4225
1b	-103.005	-71.3153
2b	-107.654	-65.0598
3b	-100.492	-77.1676
4b	-113.135	-83.6599

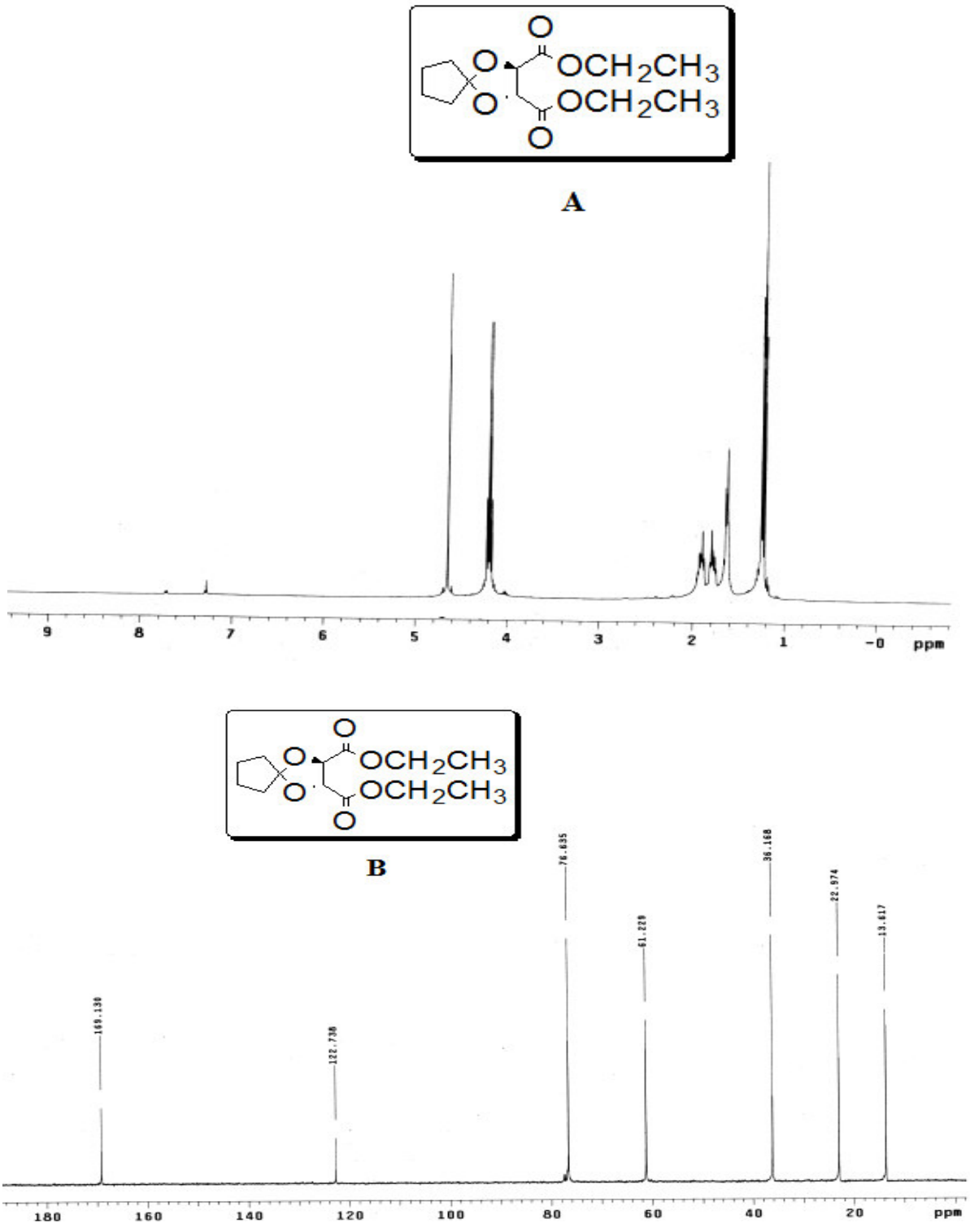

Figure S4: ^{1}H NMR (**A**) and ^{13}C NMR (**B**) of 2,3-Diethyl(2R,3R)-1,4-dioxaspiro[4.4]nonane-2,3-dicarboxylate (**6**)

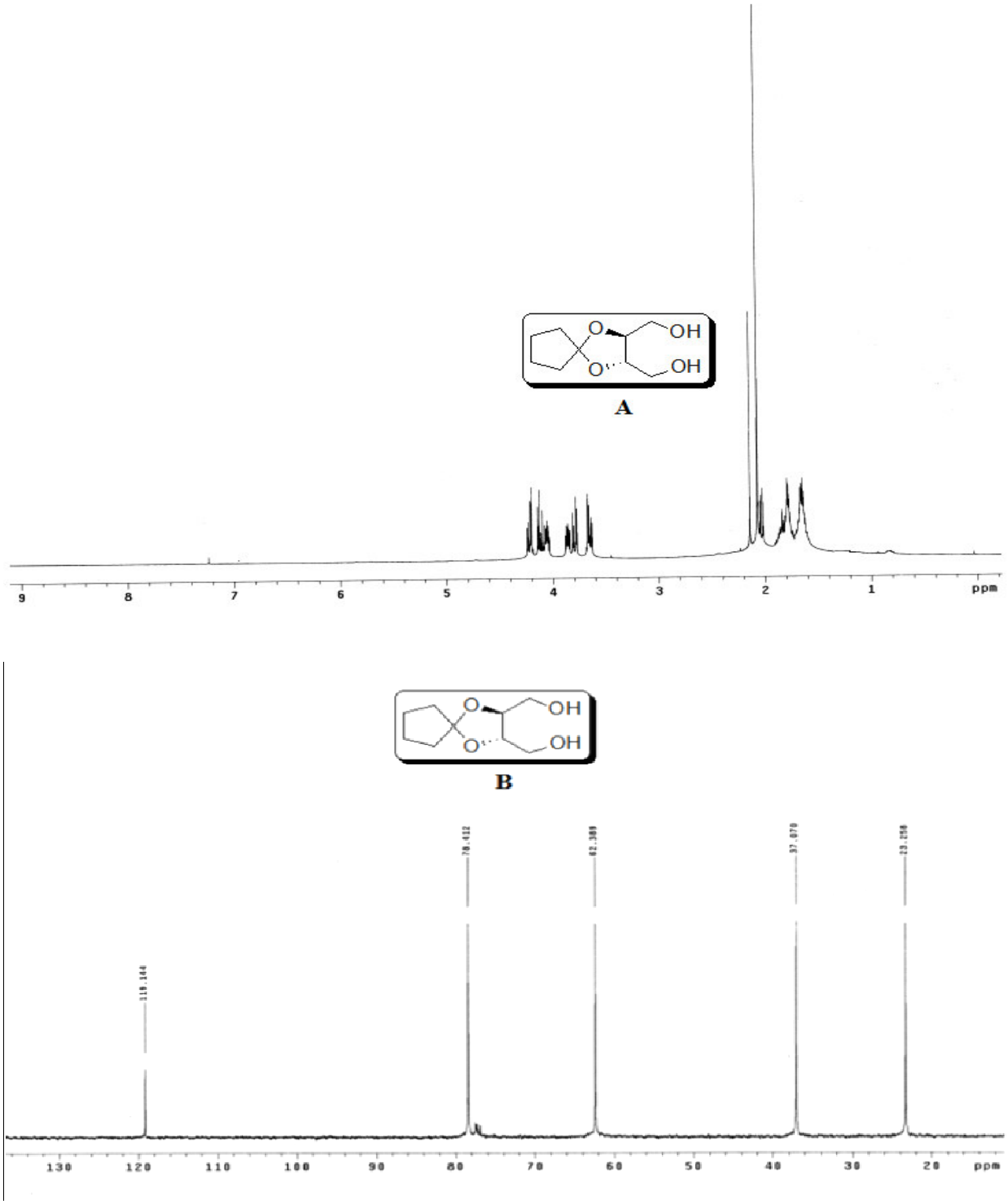

Figure S5: ^{1}H NMR (**A**) and ^{13}C NMR (**B**) of [(2S,3S)-3-(hydroxymethyl)-1,4-dioxaspiro [4.4] nonan-2-yl]methonol (**7**)

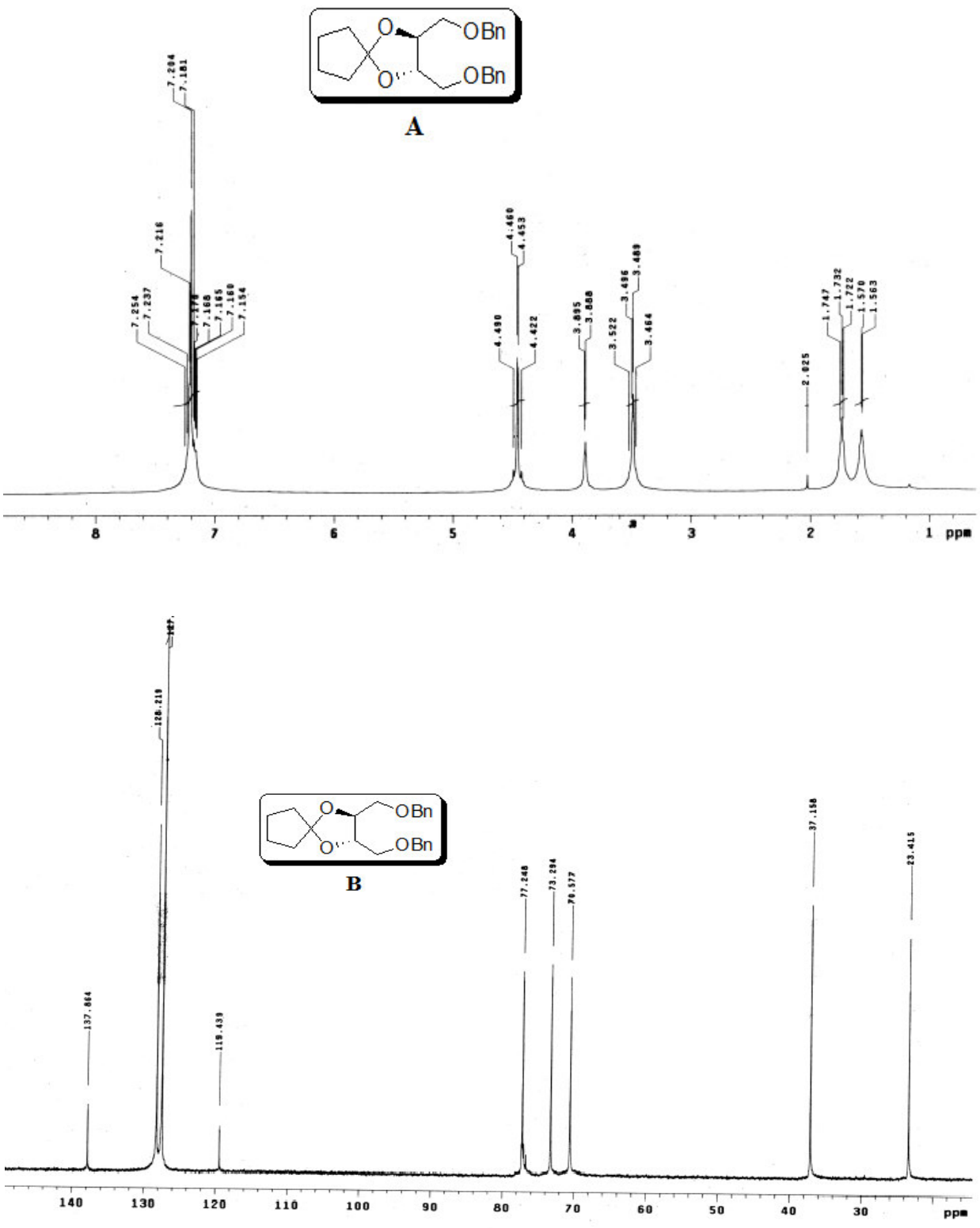

Figure S6: ^{1}H NMR (**A**) and ^{13}C NMR (**B**) of (2S,3S)-2,3-bis [(benzyloxy)methyl]-1,4-dioxaspiro[4.4]nonane (**8**)

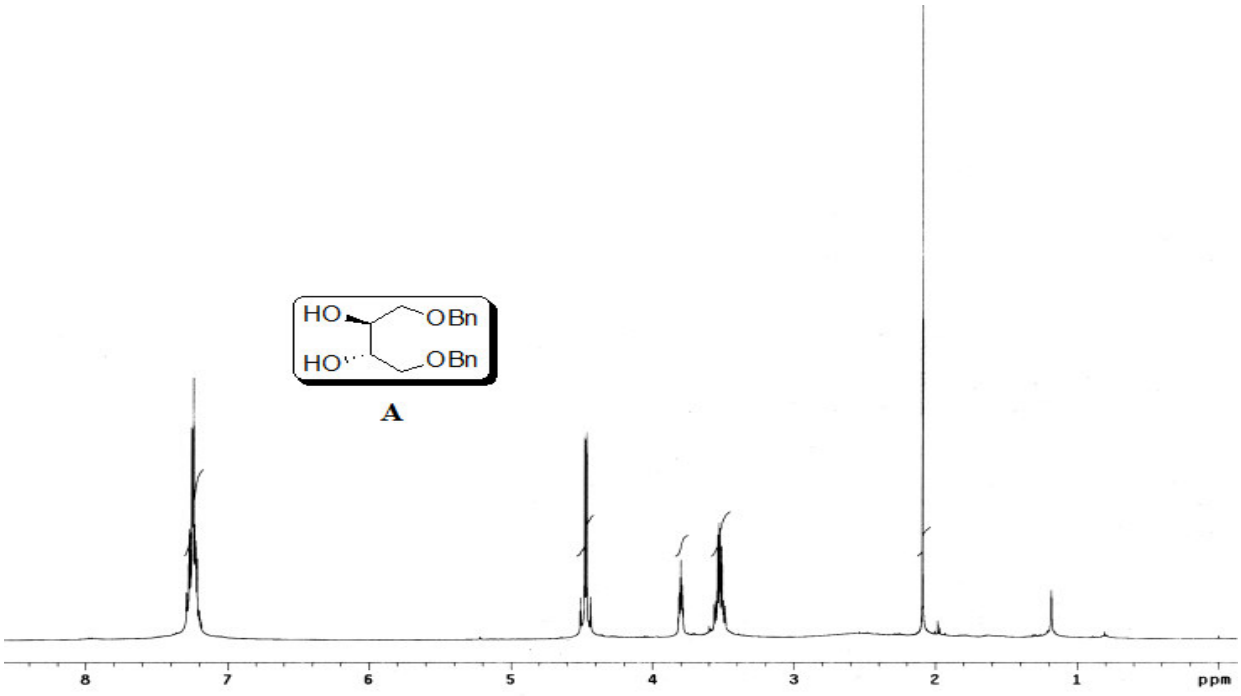

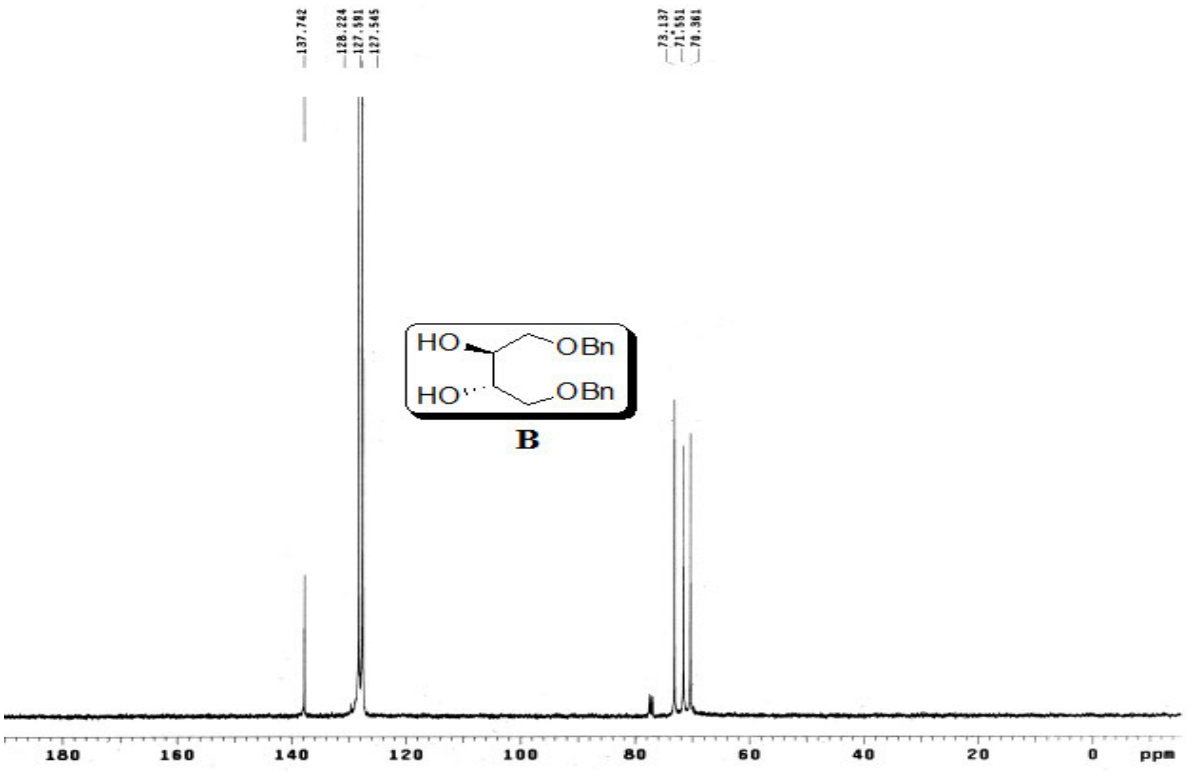

Figure S7: ^{1}H NMR (**A**) and ^{13}C NMR (**B**) of (2S,3S)-1,4-bis(benzyloxy)butane-2,3-diol (**9**)

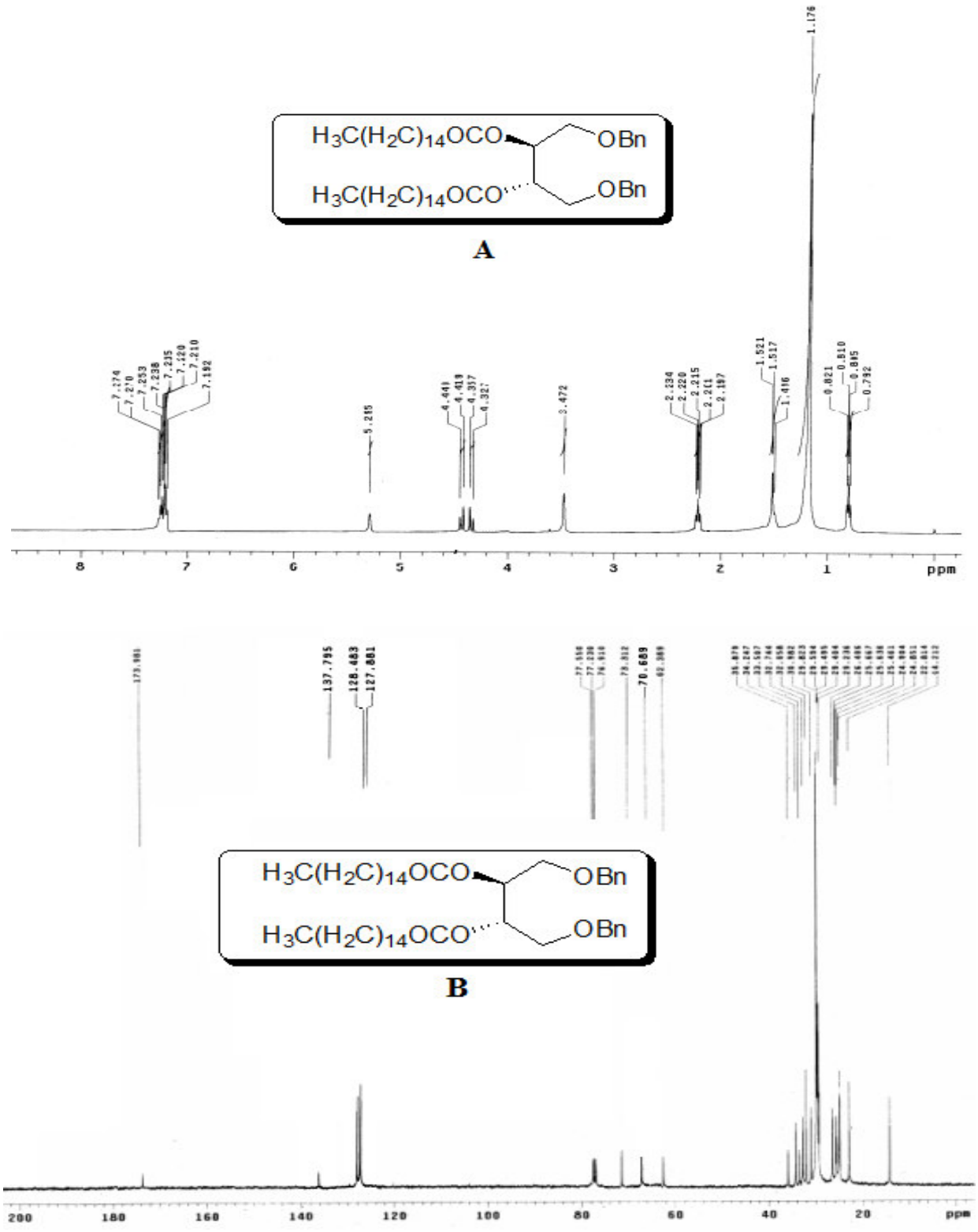

Figure S8: ^{1}H NMR (**A**) and ^{13}C NMR (**B**) of (2S,3S)-1,4-bis(benzyloxy)-3-(hexadecanoyloxy)butan-2-yl hexadecanoate (**10a**)

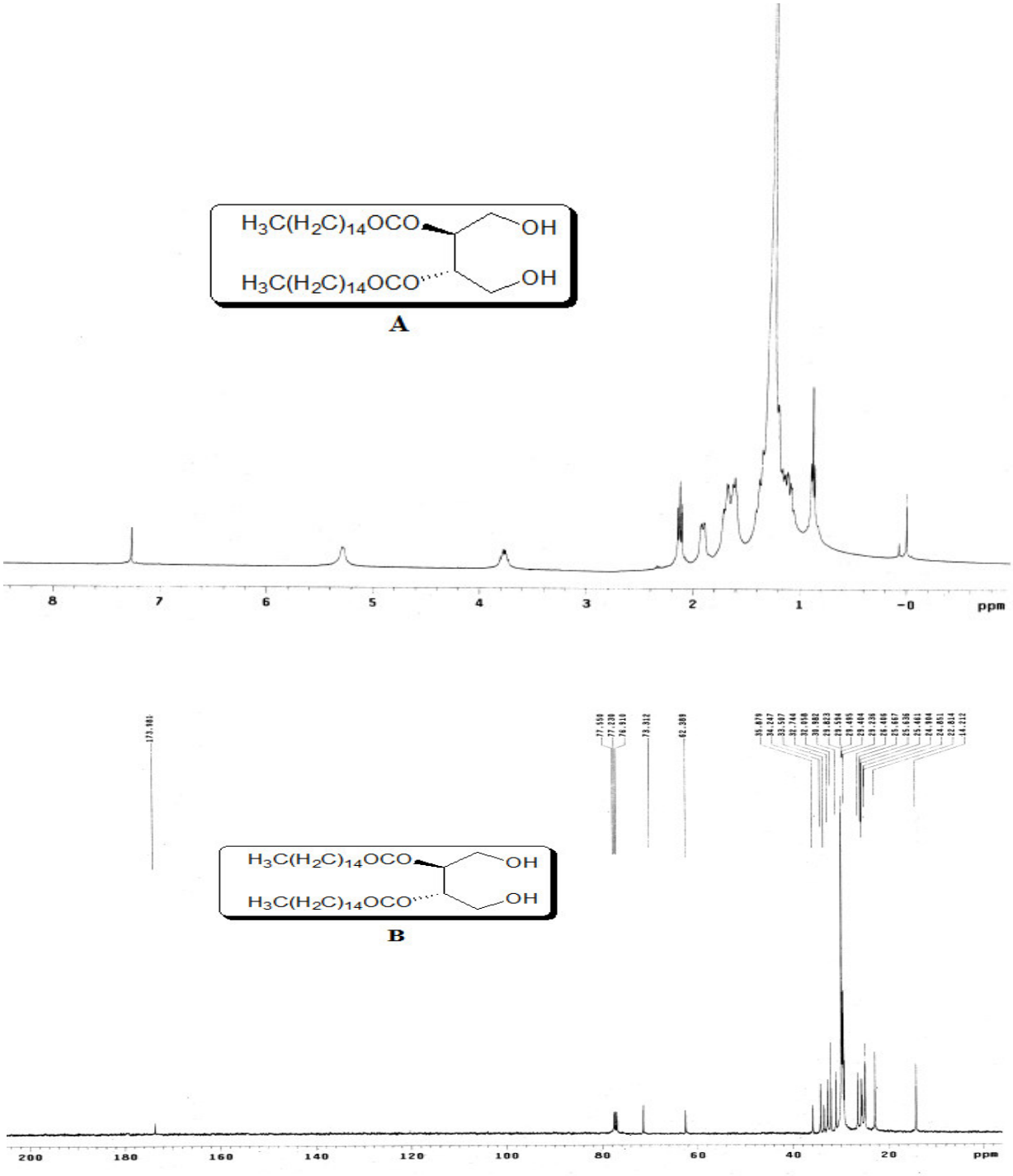

Figure S9: ^{1}H NMR (**A**) and ^{13}C NMR (**B**) of (2S,3S)-3-(hexadecanoyloxy)-1,4-dihydroxybutan-2-yl hexadecanoate (**1a**)

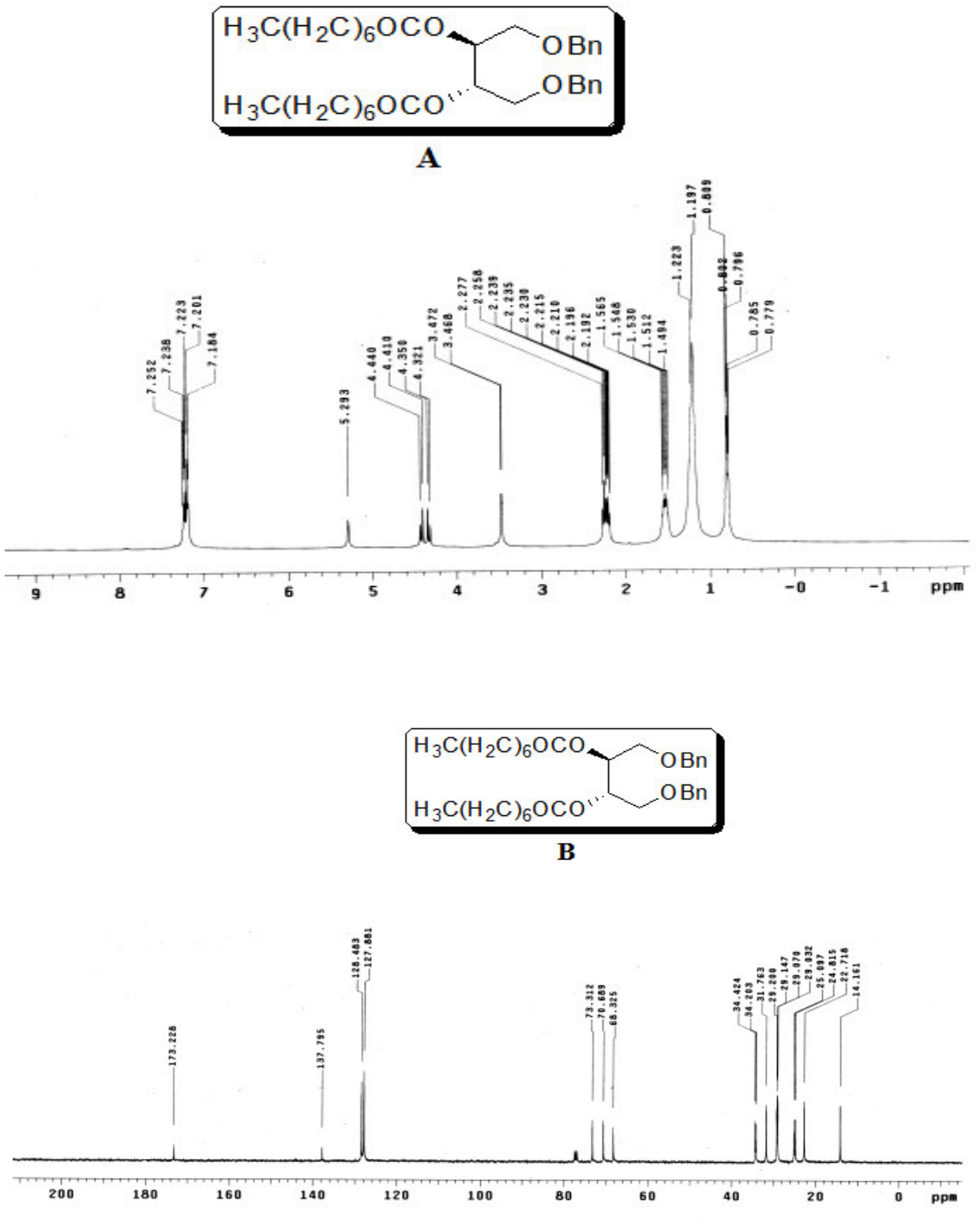

Figure S10: ^{1}H NMR (**A**) and ^{13}C NMR (**B**) of (2S,3S)-1,4-bis(benzyloxy)-3-(octanoloxy)butan-2-yl octanoate (**10b**)

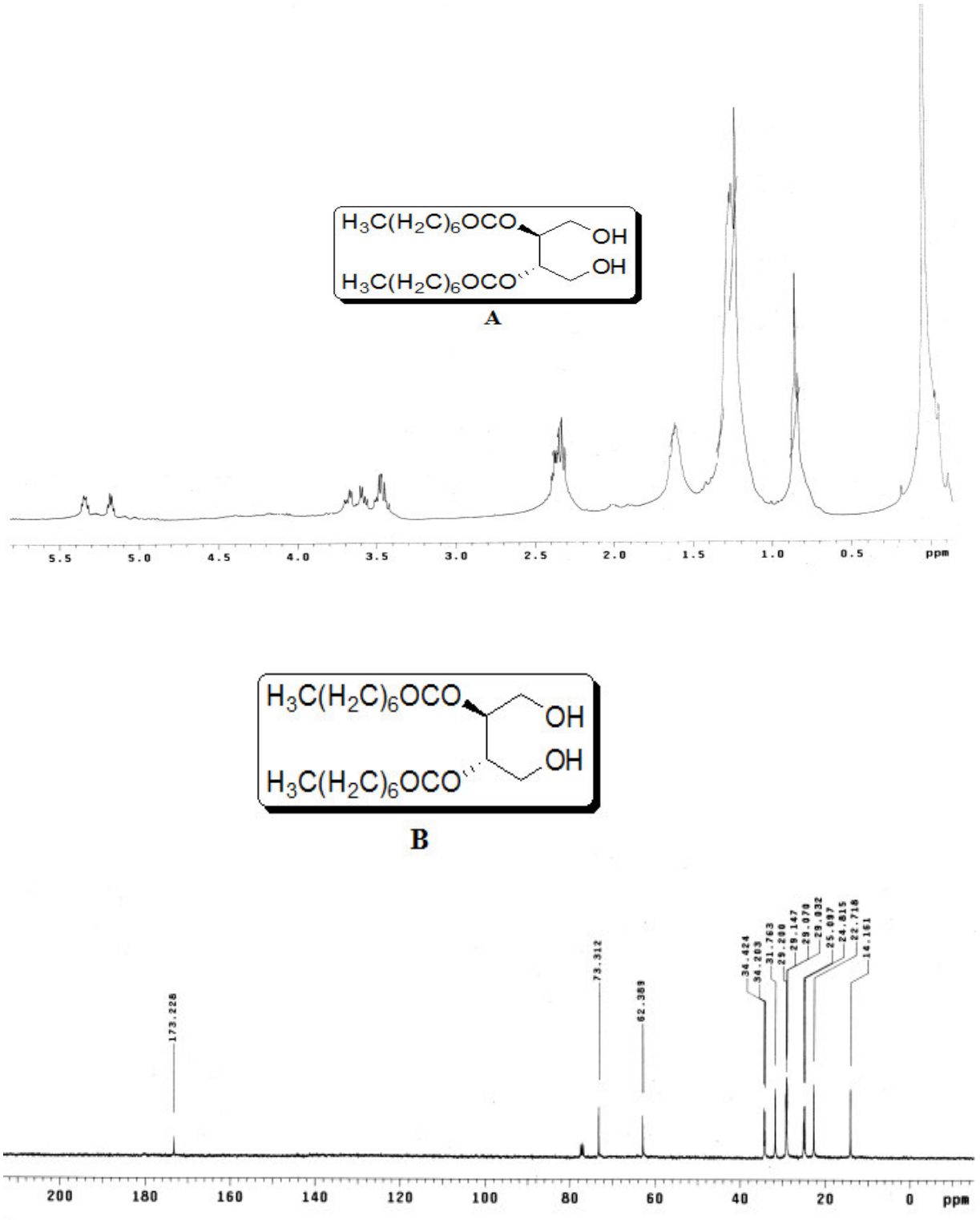

Figure S11: ^{1}H NMR (**A**) and ^{13}C NMR (**B**) of (2S,3S)-1,4-dihydroxy-3-(octanoloxy)butan-2-yl octanoate (**1b**)

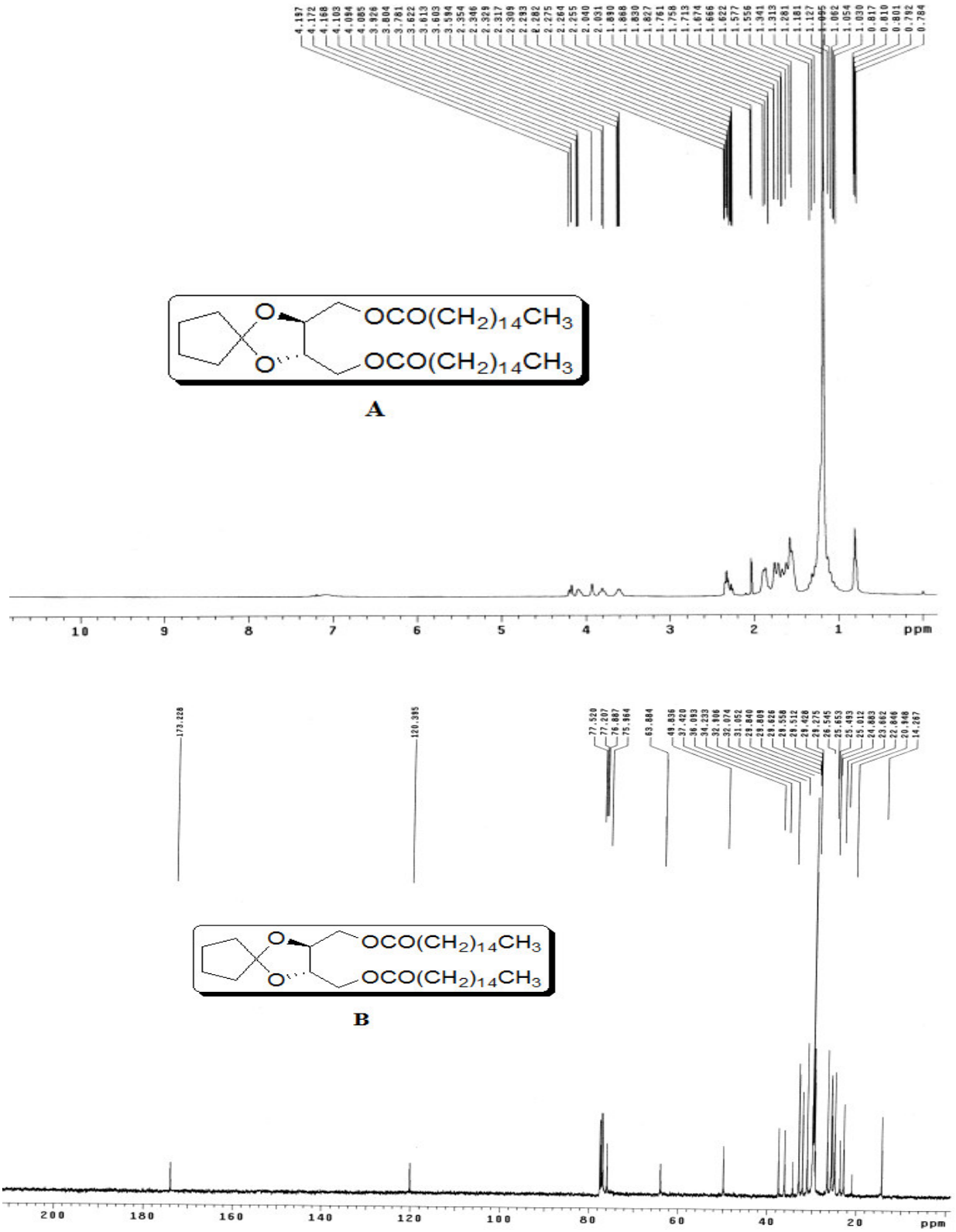

Figure S12: ^{1}H NMR (**A**) and ^{13}C NMR (**B**) of [(2S,3S)-3-[(hexadecanoyloxy)methyl]-1,4-dioxapiro[4.4]nonan-2-yl]methyl hexadecanoate (**11a**)

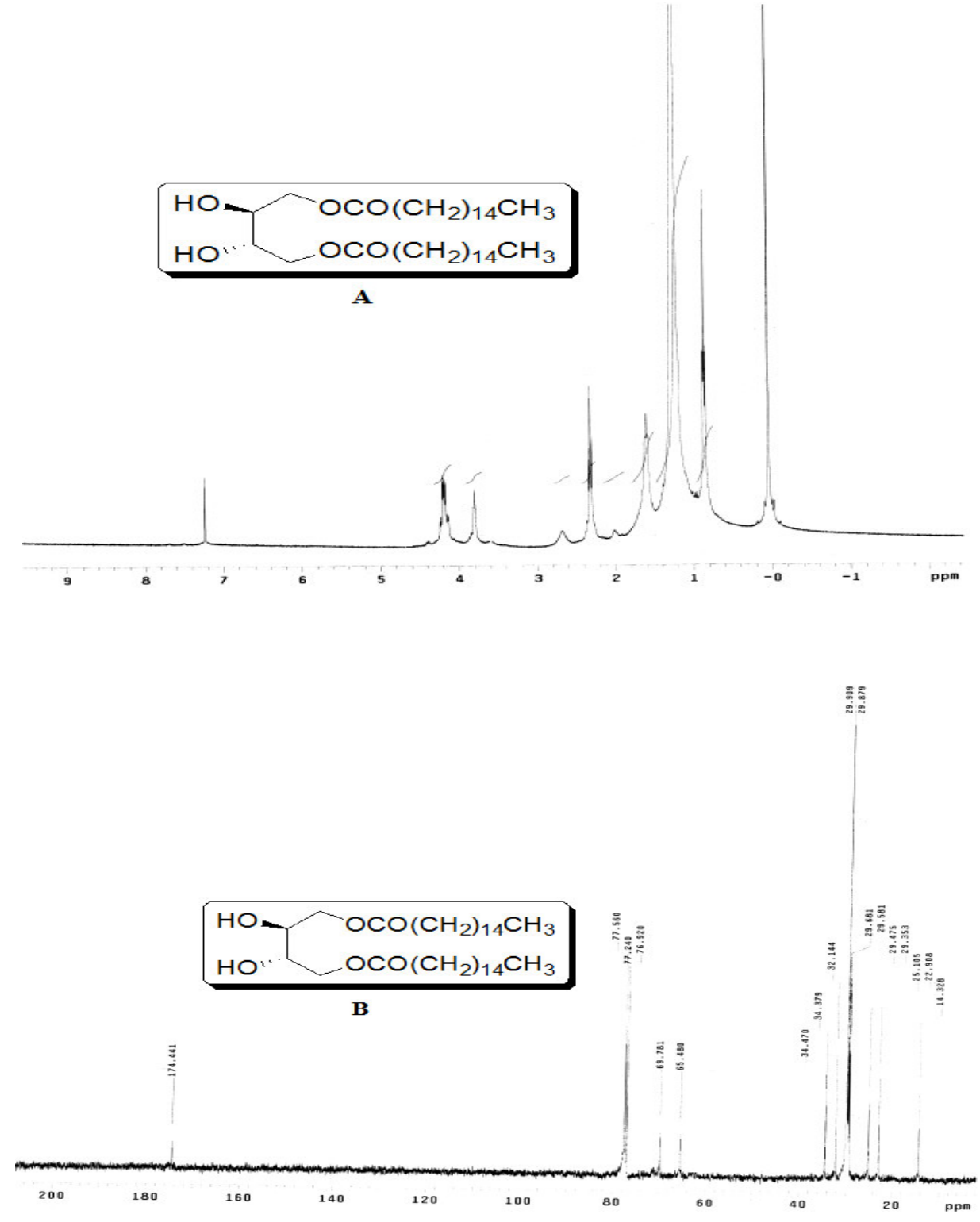

Figure S13: ^{1}H NMR (**A**) and ^{13}C NMR (**B**) of (2S,3S)-4-hexadecanoloxy-2,3-dihydroxybutyl hexadecanoate (**2a**)

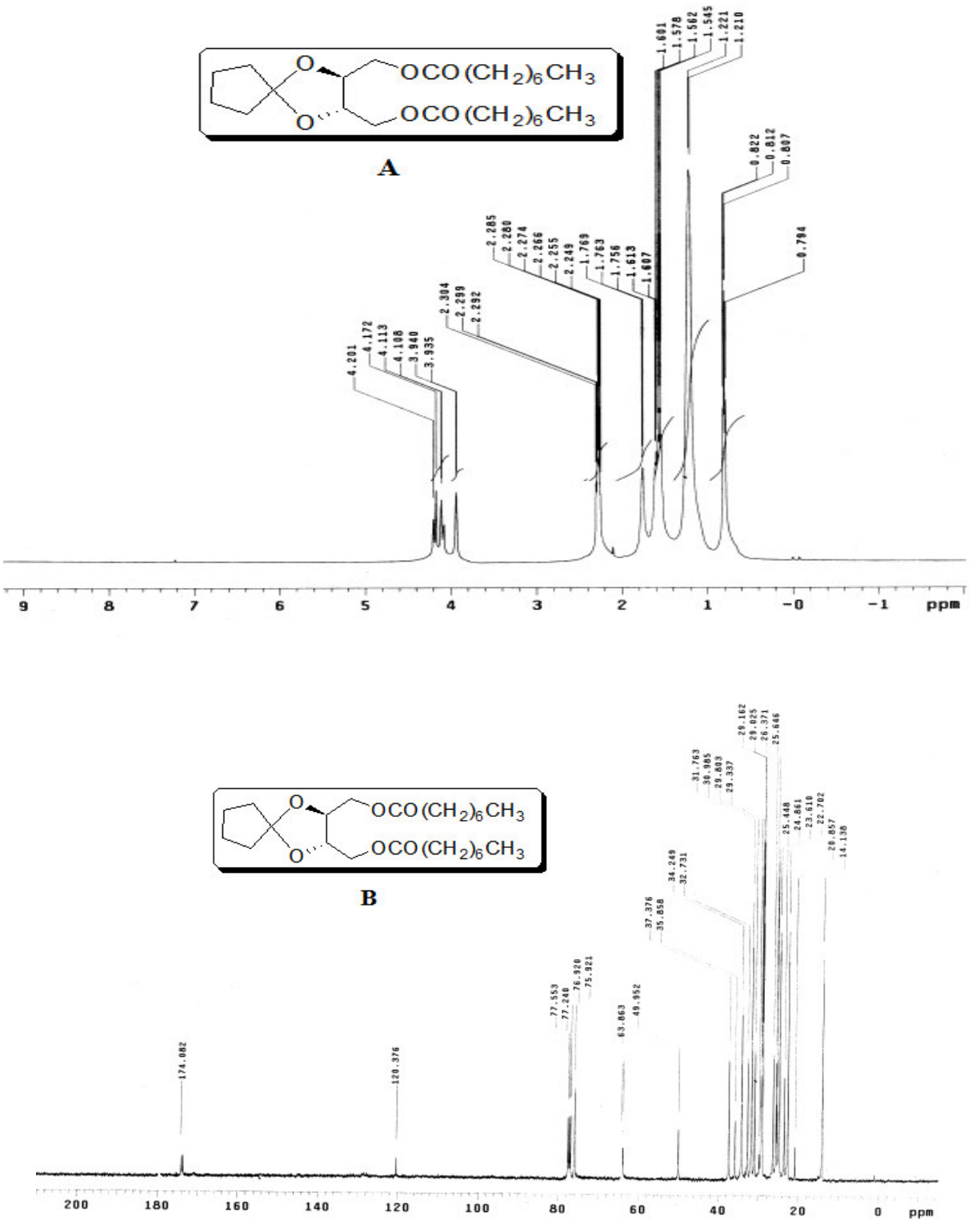

Figure S14: ^{1}H NMR (**A**) and ^{13}C NMR (**B**) of [(2S,3S)-3-[(octanoyloxy) methyl]-1,4-dioxapiro [4.4]nonan-2-yl] methyl octanoate (**11b**)

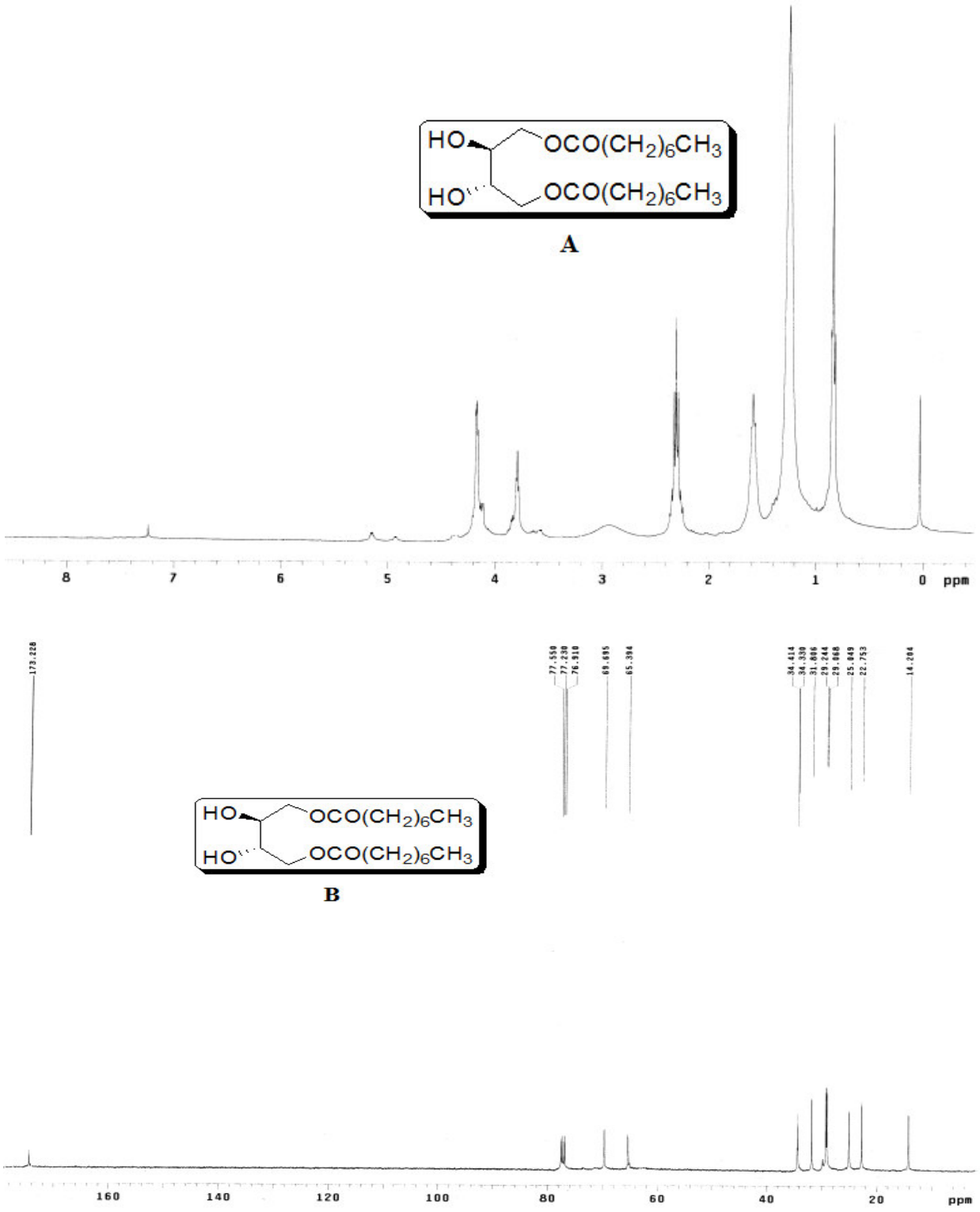

Figure S15: ^{1}H NMR (**A**) and ^{13}C NMR (**B**) of (2S,3S)-2,3-dihydroxy-4-(octanoloxy)butyloctanoate (**2b**)

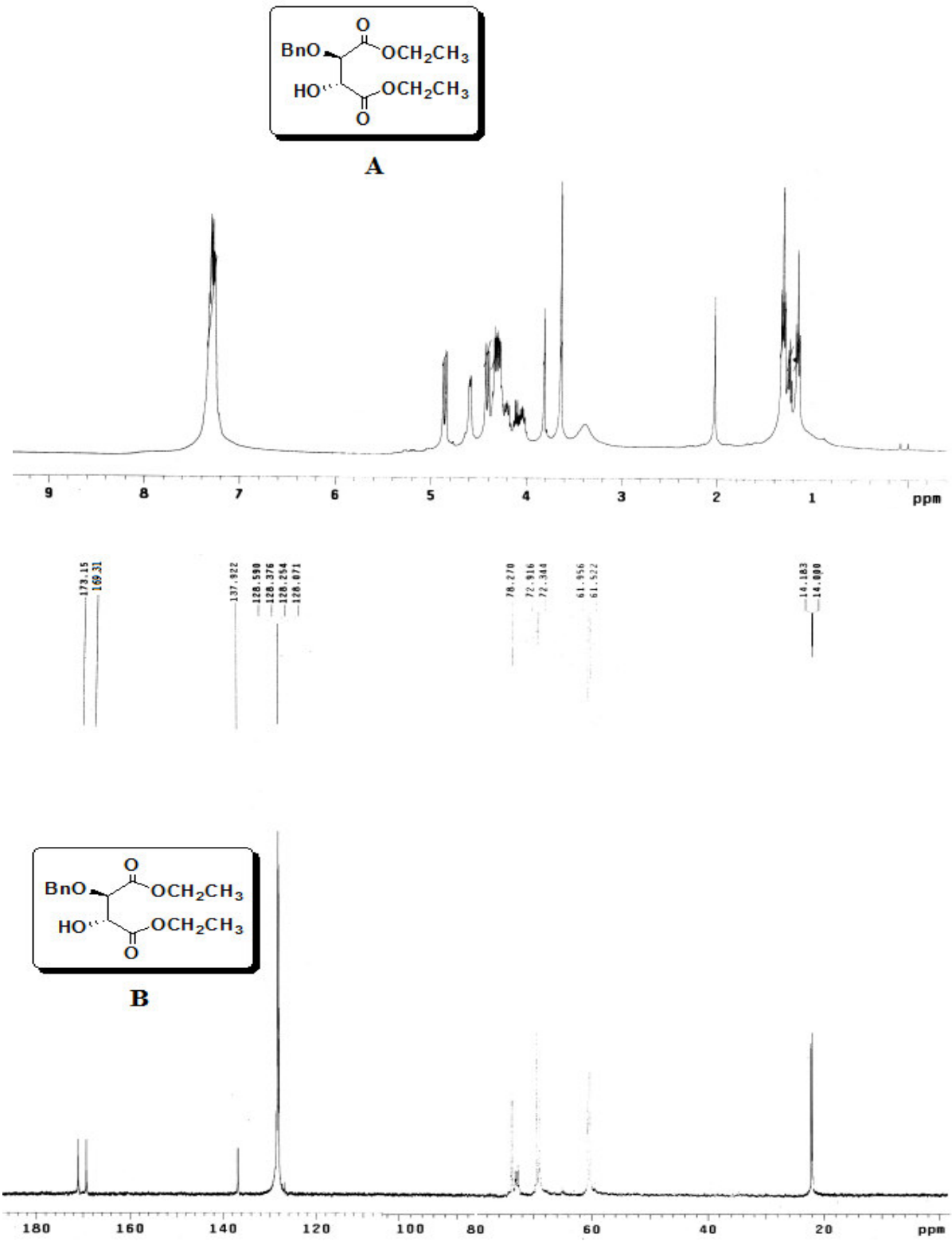

Figure S16: ^{1}H NMR (**A**) and ^{13}C NMR (**B**) of (2R,3R)-diethyl 2-(benzyloxy)-3-hydroxy succinate (**12**)

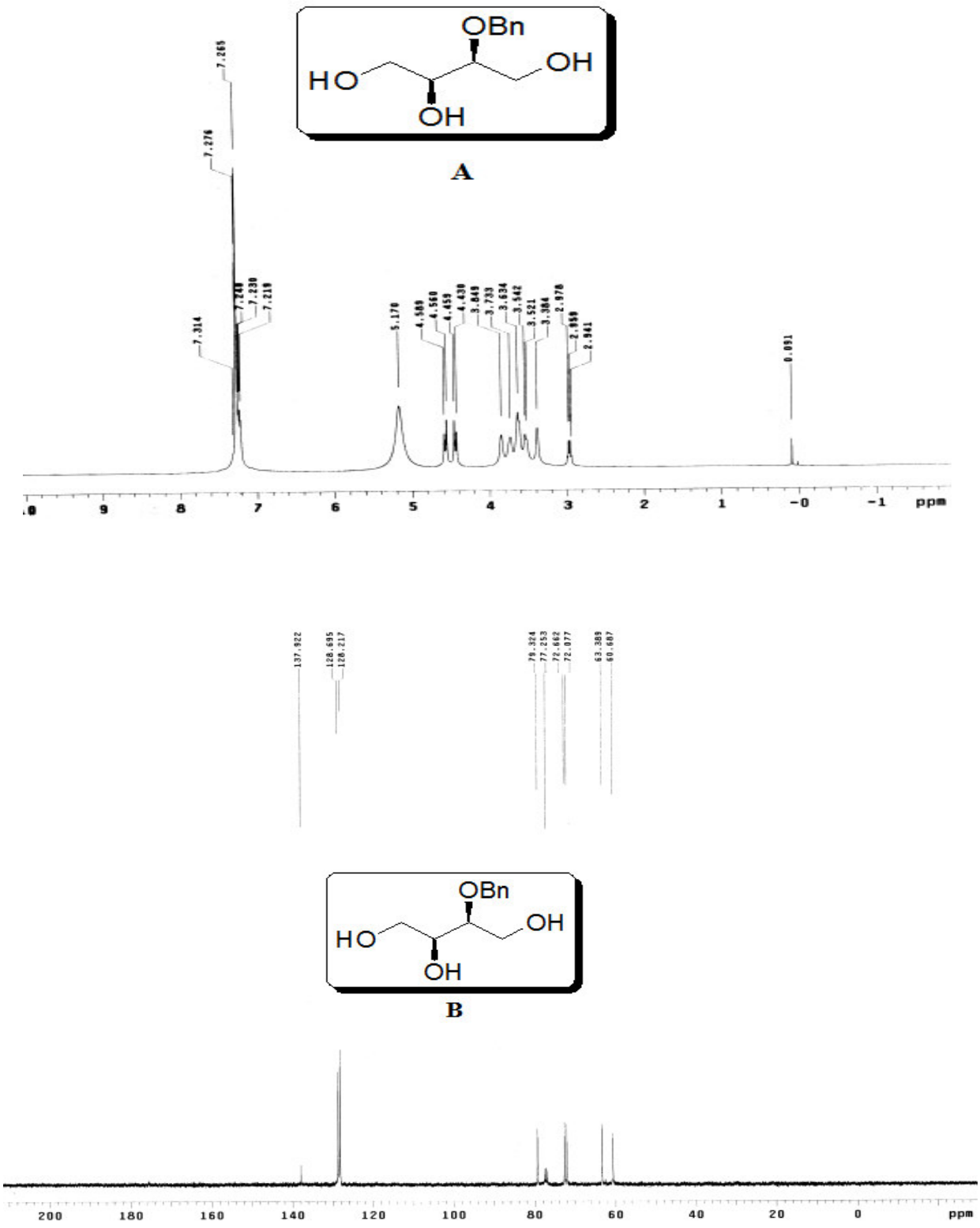

Figure S17: ^{1}H NMR (**A**) and ^{13}C NMR (**B**) of (2S,3S)-3-(benzyloxy)-1,2,4-triol (**13**)

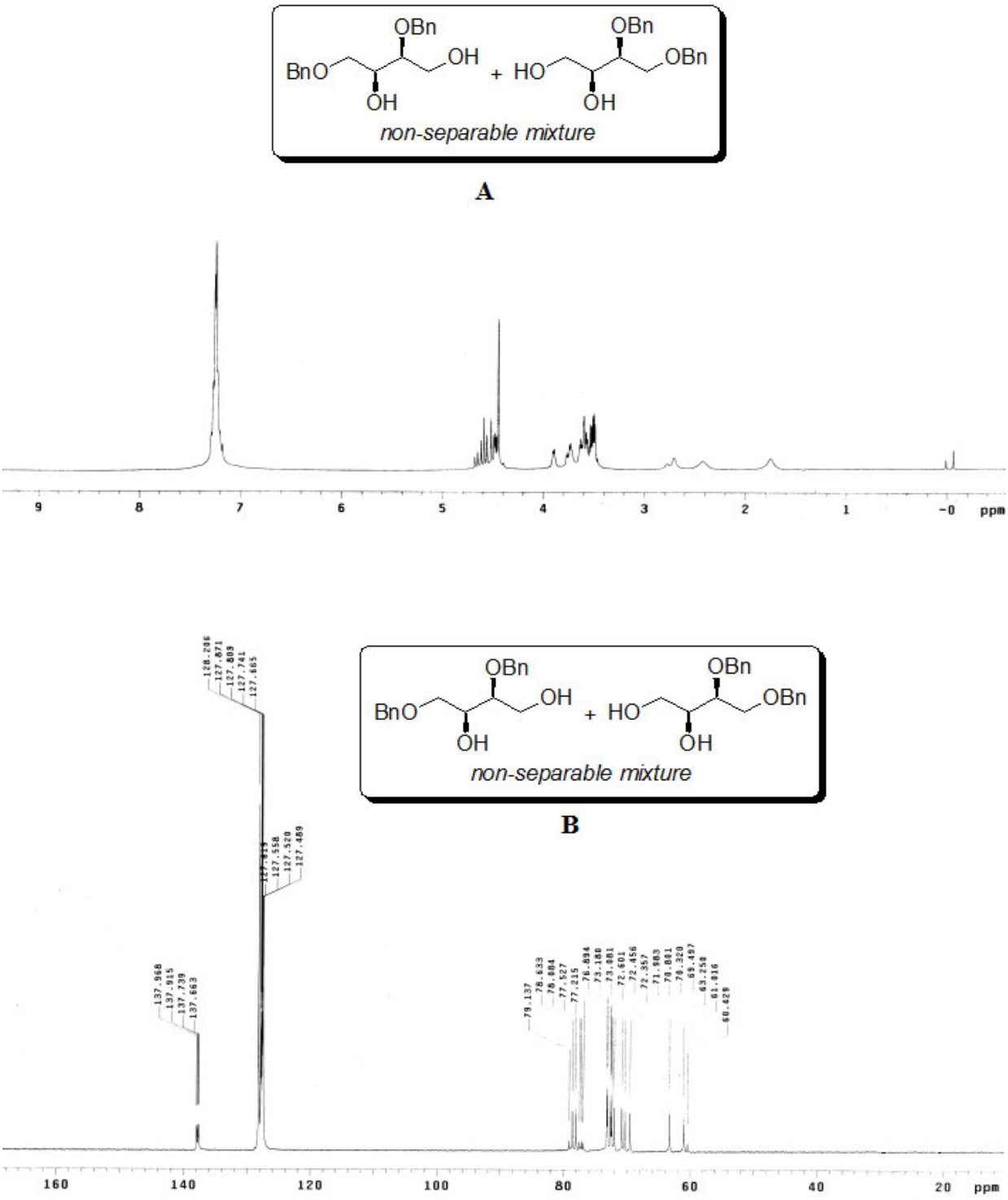

Figure S18: ^{1}H NMR (**A**) and ^{13}C NMR (**B**) of (2S,3S)2,4-bis (benzyloxy) butane-1,3-diol & (2S,3S)3 4-bis (benzyloxy) butane-1,2-diol (**14** and **15**)

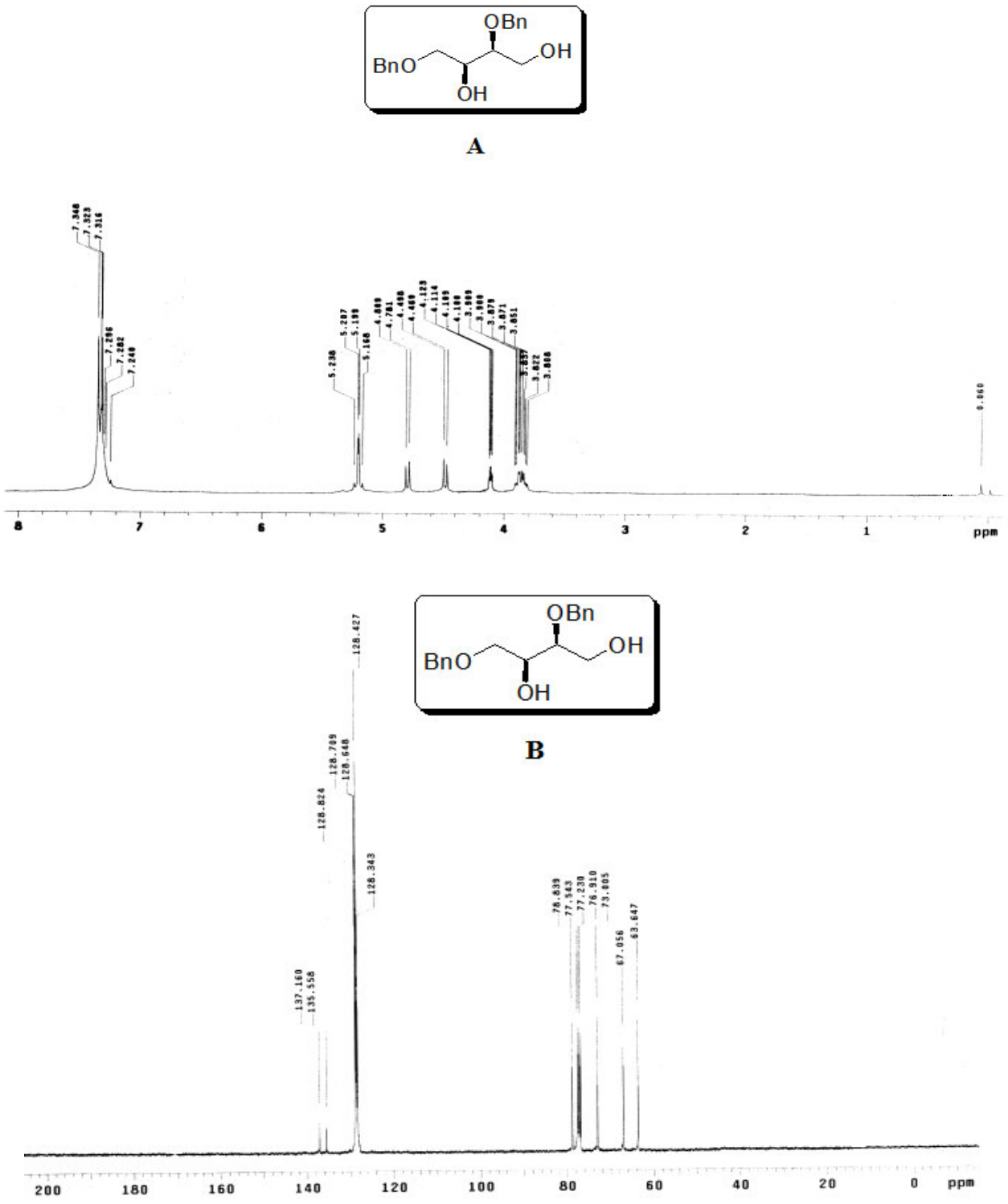

Figure S19: ^{1}H NMR (**A**) and ^{13}C NMR (**B**) of (2S,3S)-2,4-bis (benzyloxy)butane-1,3-diol (**15**)

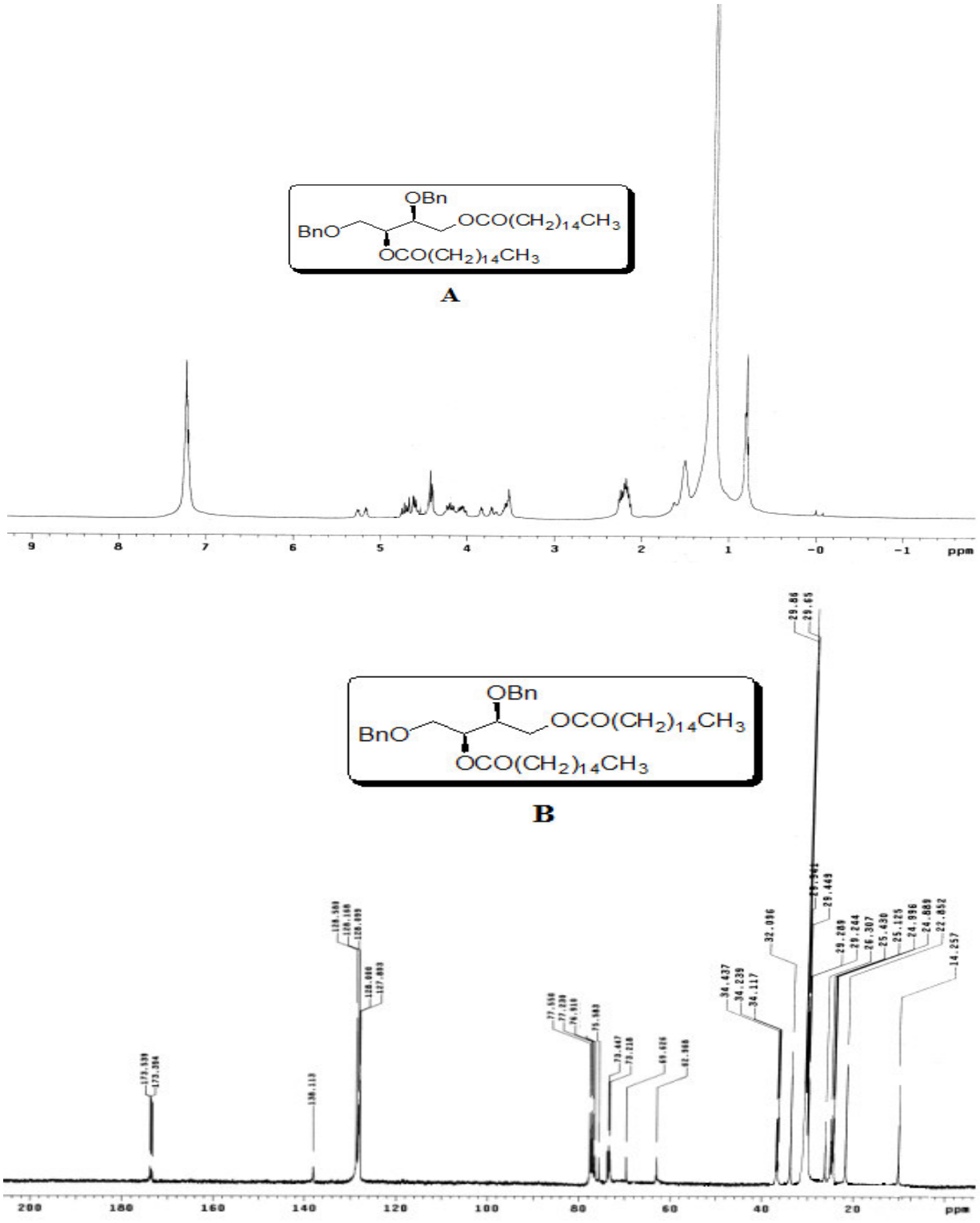

Figure S20: ^{1}H NMR (**A**) and ^{13}C NMR (**B**) of (2S,3S)-1,3-bis(benzyloxy)-4-(hexadecanoyloxy)butan-2-yl hexadecanoate (**17a**)

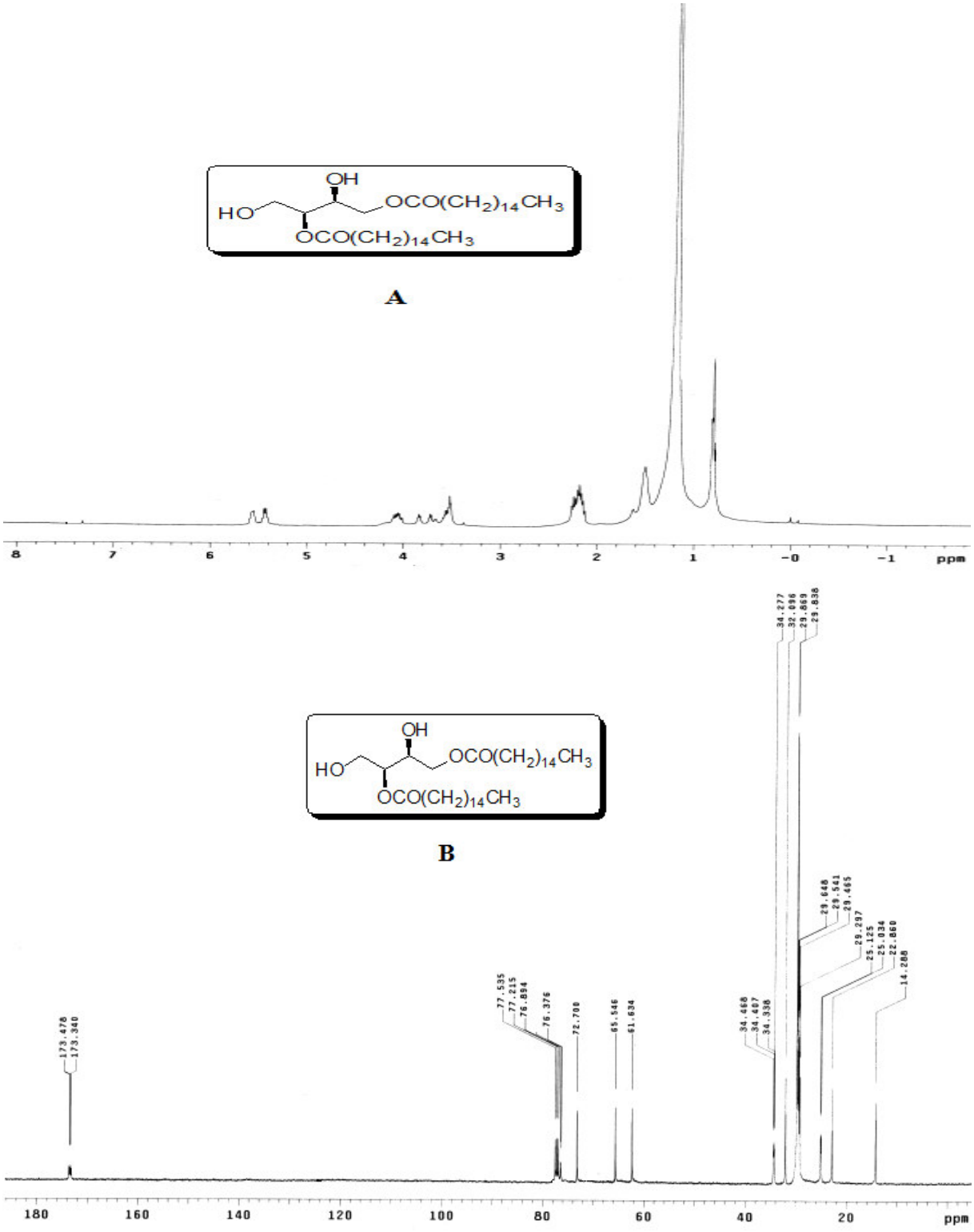

Figure S21: ^{1}H NMR (**A**) and ^{13}C NMR (**B**) of (2S,3S)-4-(hexadecanoyloxy)-1,3-dihydroxybutan-2-yl hexadecanoate (**3a**)

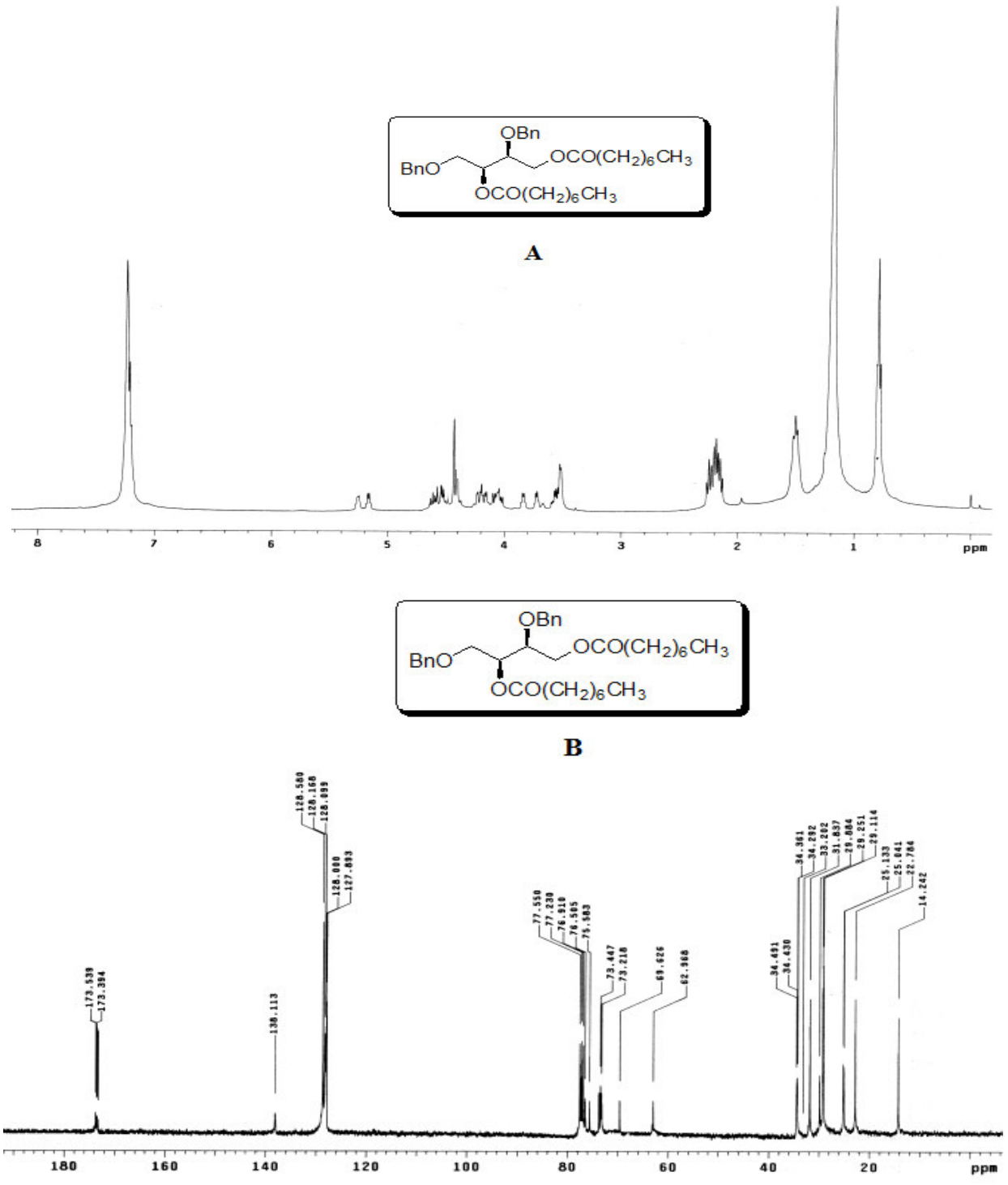

Figure S22: ^{1}H NMR (**A**) and ^{13}C NMR (**B**) of (2S,3S)-1,3-bis(benzyloxy)-4-(octanoyloxy)butan-2-yl octanoate (**17b**)

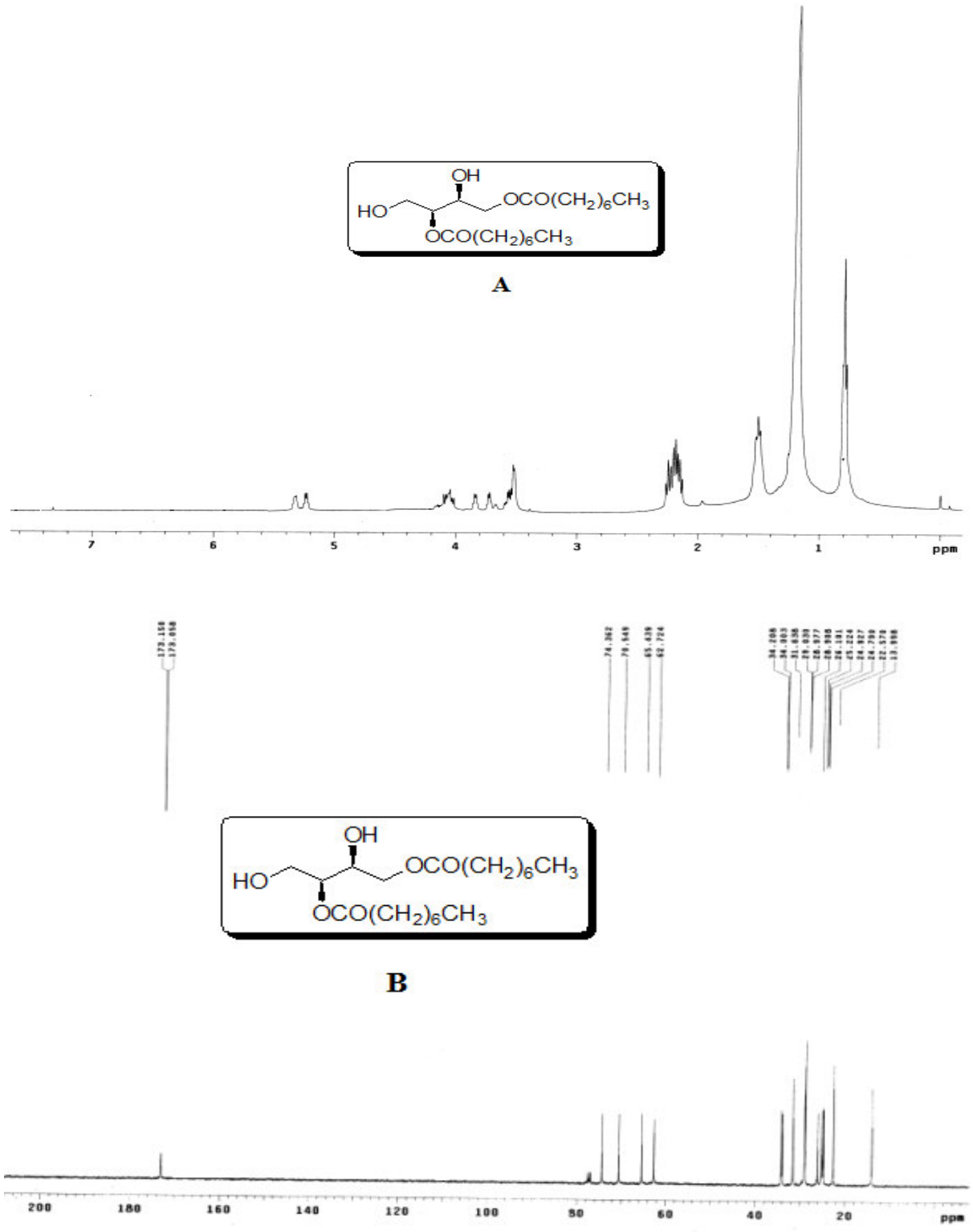

Figure S23: ^{1}H NMR (**A**) and ^{13}C NMR (**B**) of (2S,3S)-1,3-dihydroxy-4-(octanoyloxy)butane-2-yl octanoate (**3b**)

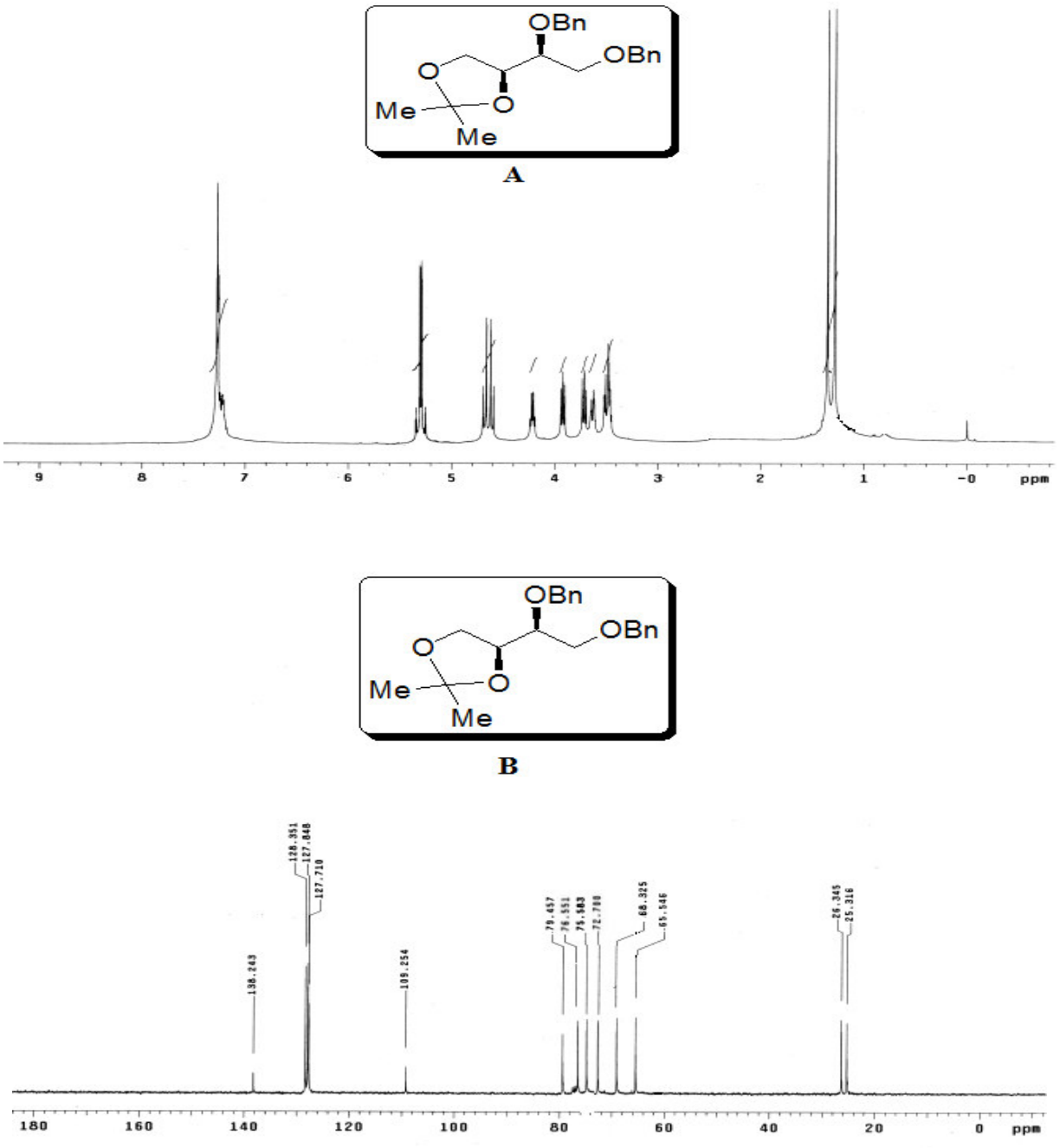

Figure S24: ^{1}H NMR (**A**) and ^{13}C NMR (**B**) of (4S)-4-[(1S)-1,2-bis (benzyloxy) ethyl]-2,2 dimethyl-1,3-dioxolane (**16**)

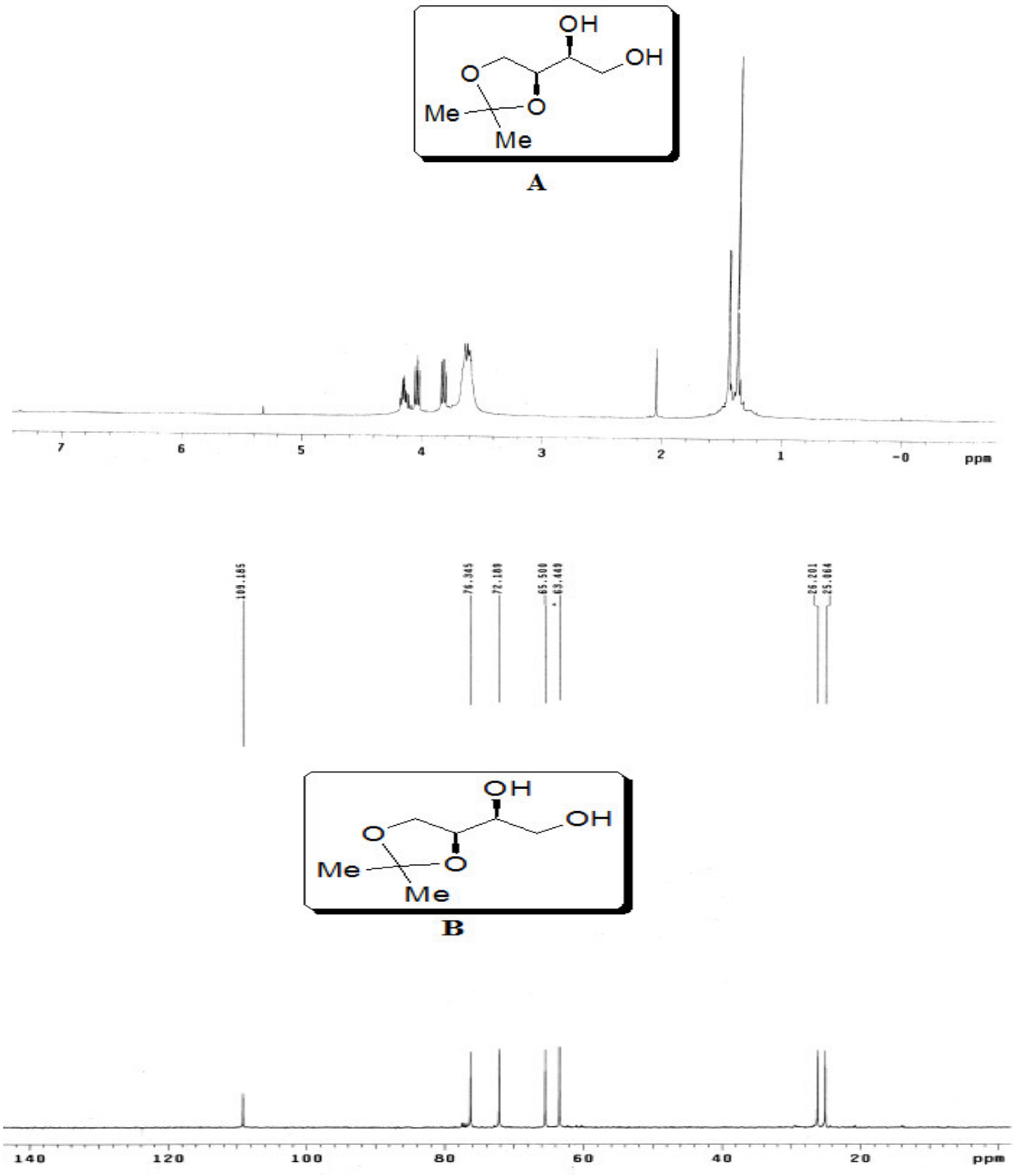

Figure S25: ^{1}H NMR (**A**) and ^{13}C NMR (**B**) of (1S)-1-[(4S)-2,2-dimethyl-1,3-dioxolan-4yl]ethane-1,2-diol (**18**)

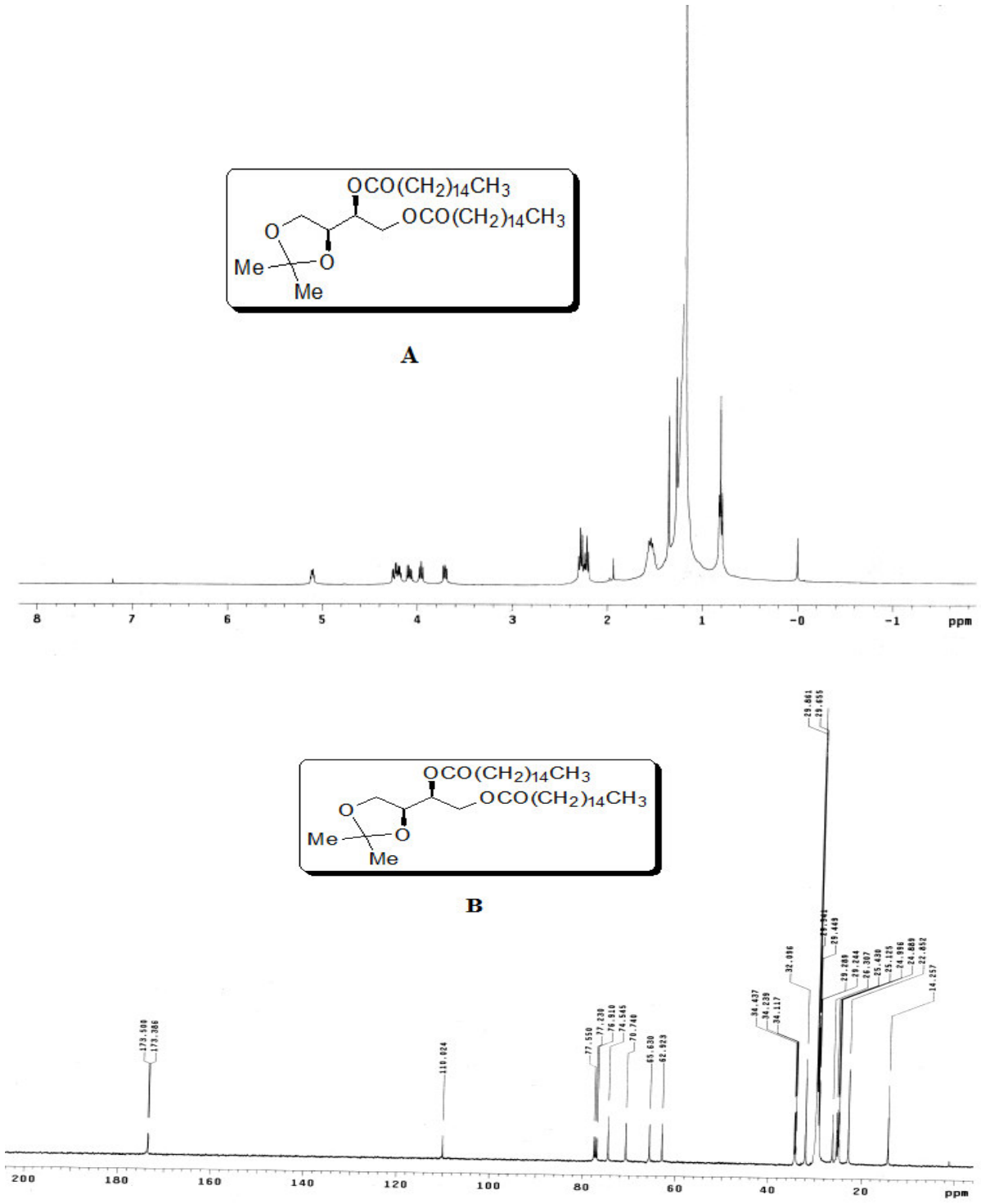

Figure S26: ^{1}H NMR (**A**) and ^{13}C NMR (**B**) of (1S)-1-[(4S)-2,2-dimethyl-1,3-dioxan-4-yl]-2-(hexadecanoyloxy)ethyl hexadecanoate(**19a**)

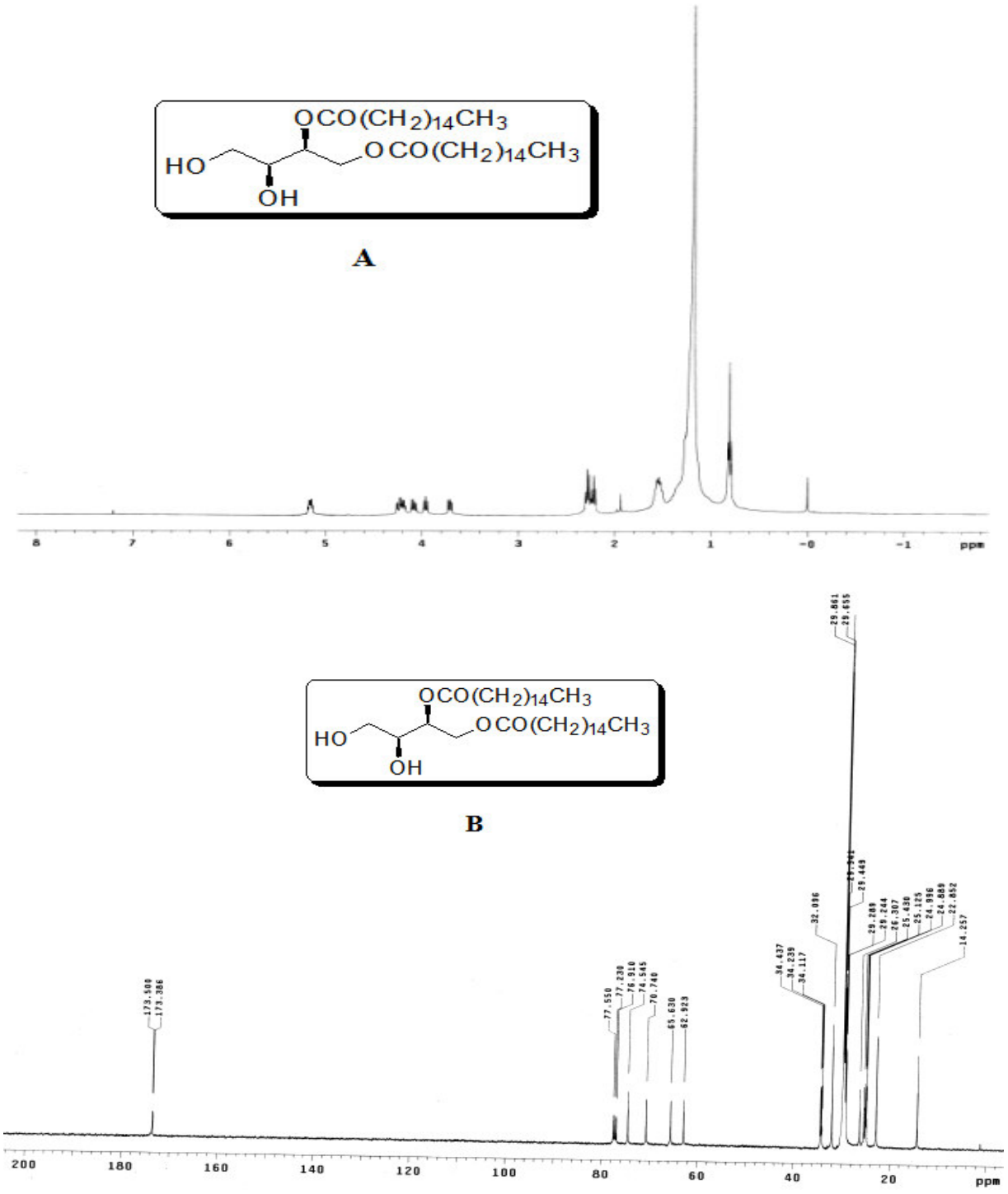

Figure S27: ^{1}H NMR (**A**) and ^{13}C NMR (**B**) of (2S,3S)-1-(hexadecanoyloxy)-3,4-dihydroxybutan-2-yl-hexadecanoate (**4a**)

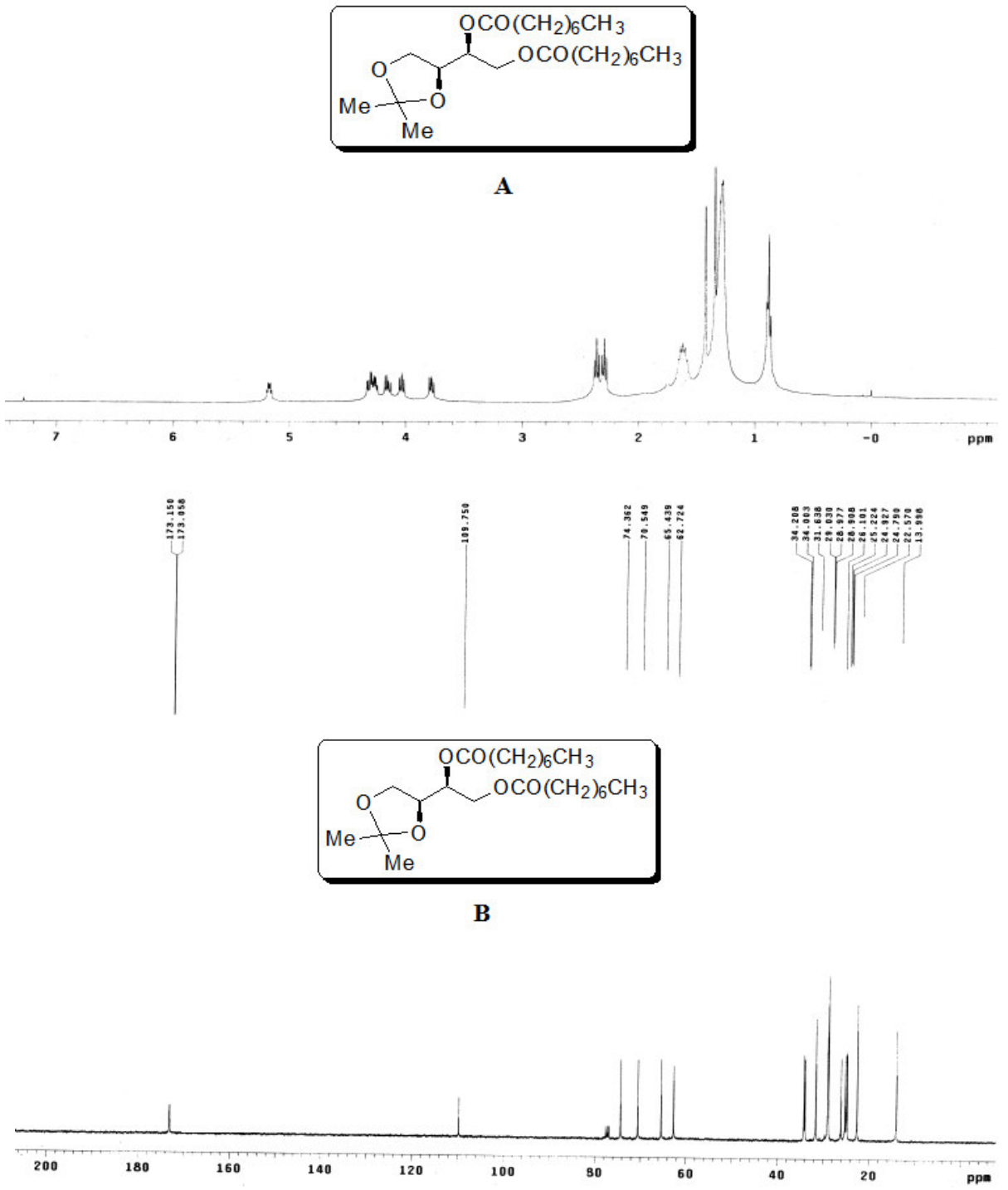

Figure S28: ^{1}H NMR (**A**) and ^{13}C NMR (**B**) of (1S)-1-[(4S)-2,2-dimethyl-1,3-dioxolan-4-yl]-2-(octanoyloxy)ethyl octanoate (**19b**)

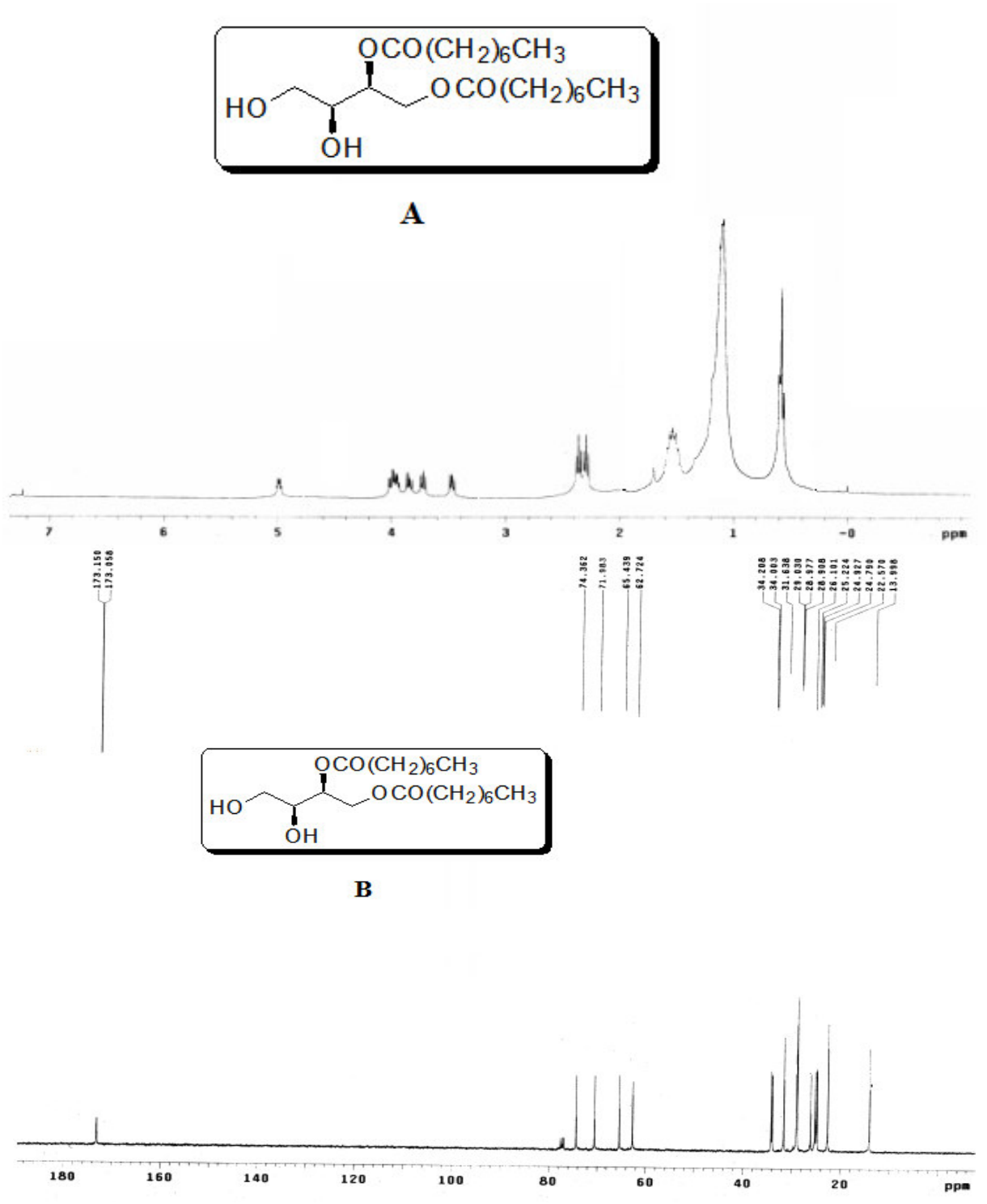

Figure S29: ^{1}H NMR (**A**) and ^{13}C NMR (**B**) of (2S,3S)-3,4-dihydroxy-1-(ocatnoyloxy)butane-2-yl octanoate (**4b**)

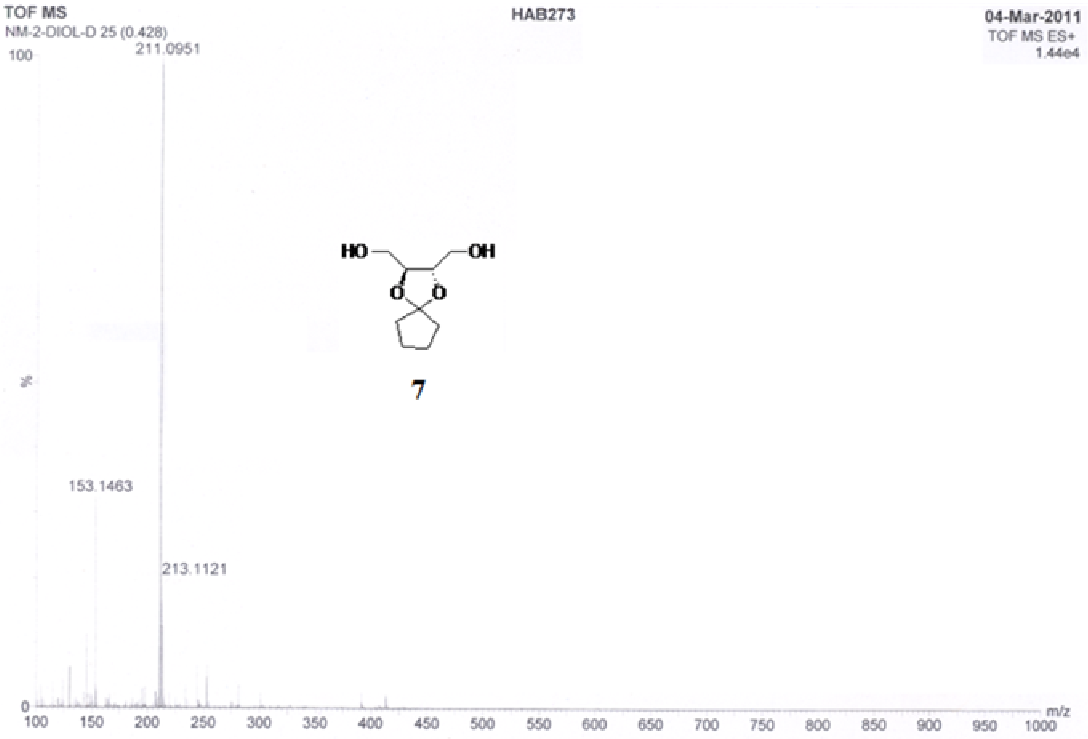

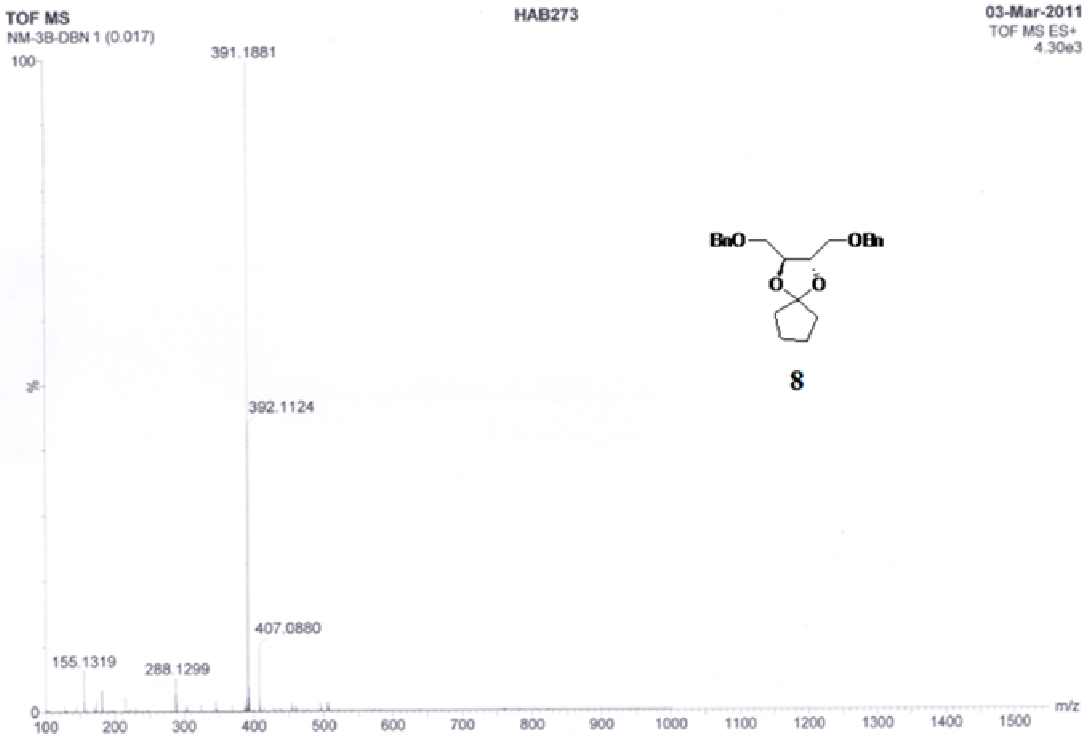

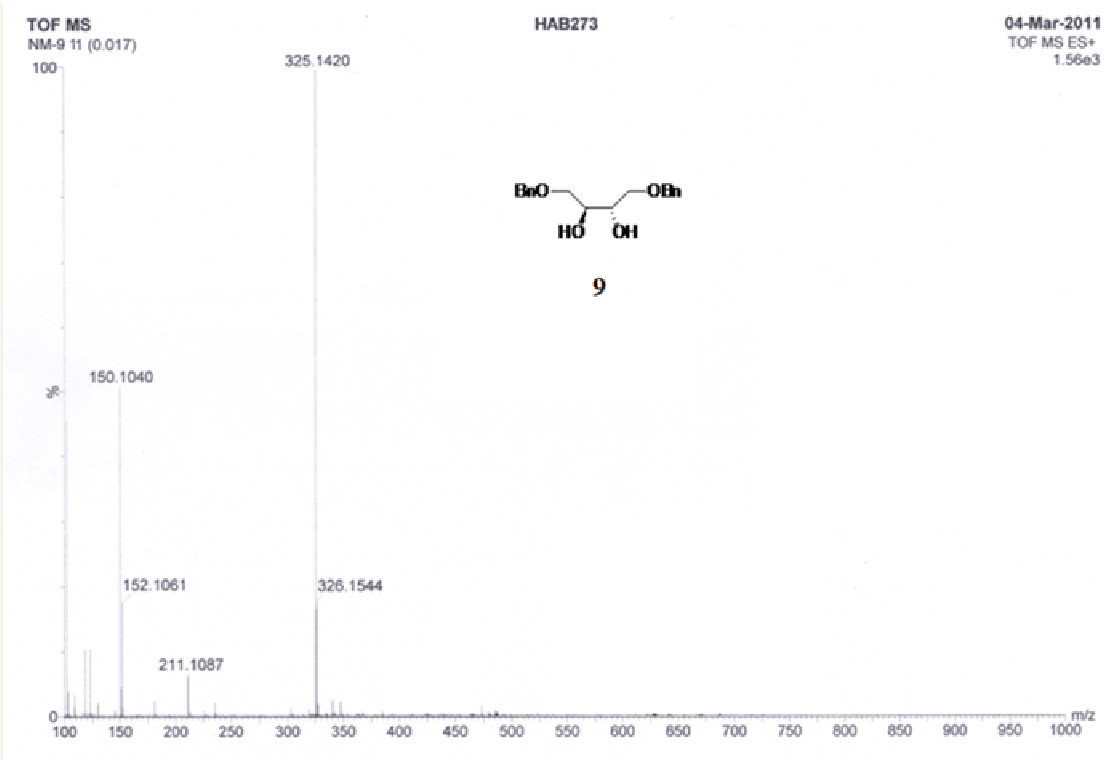

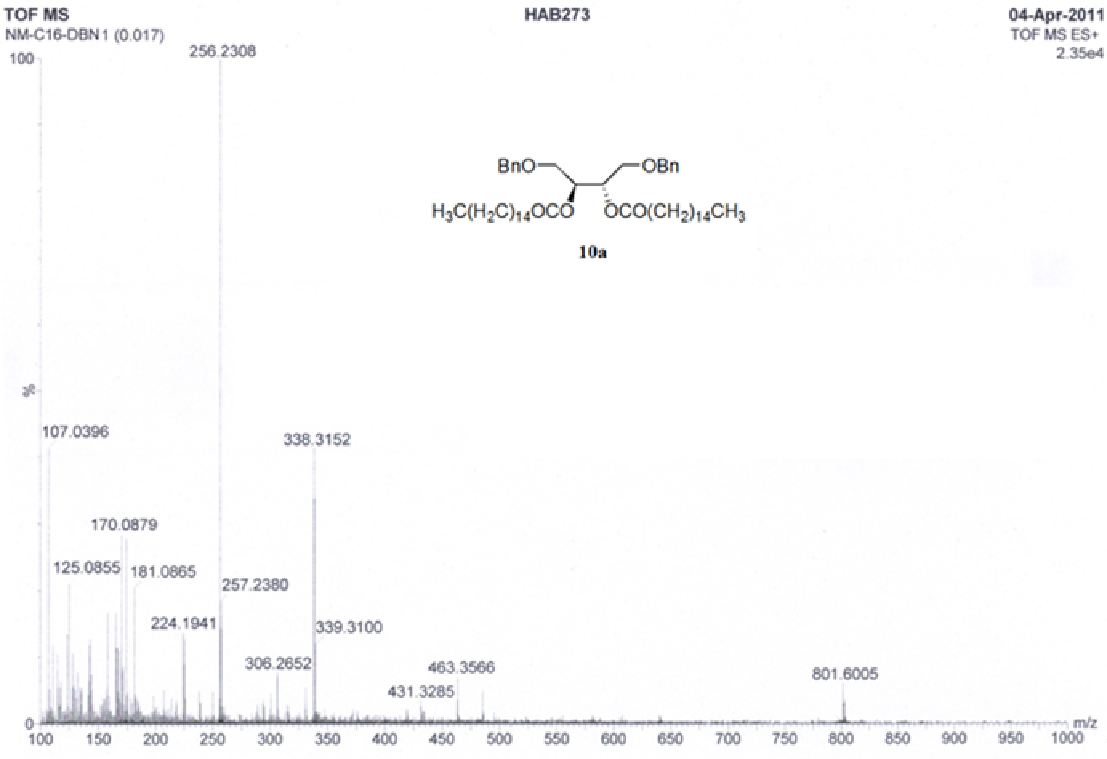

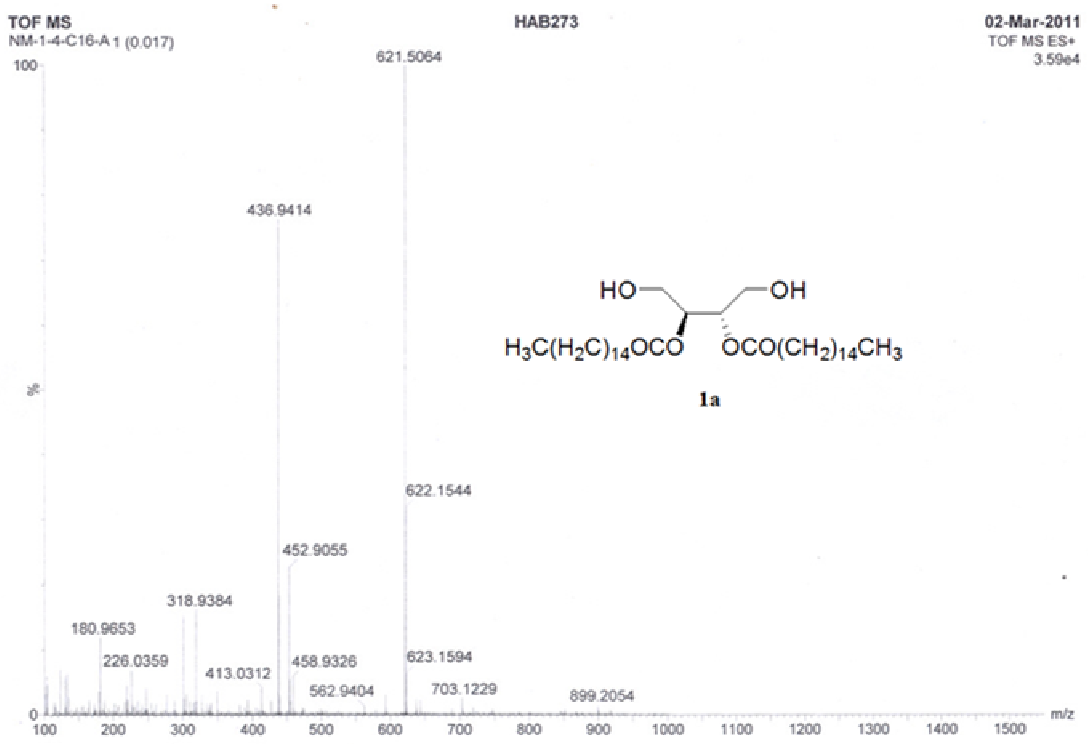

1a

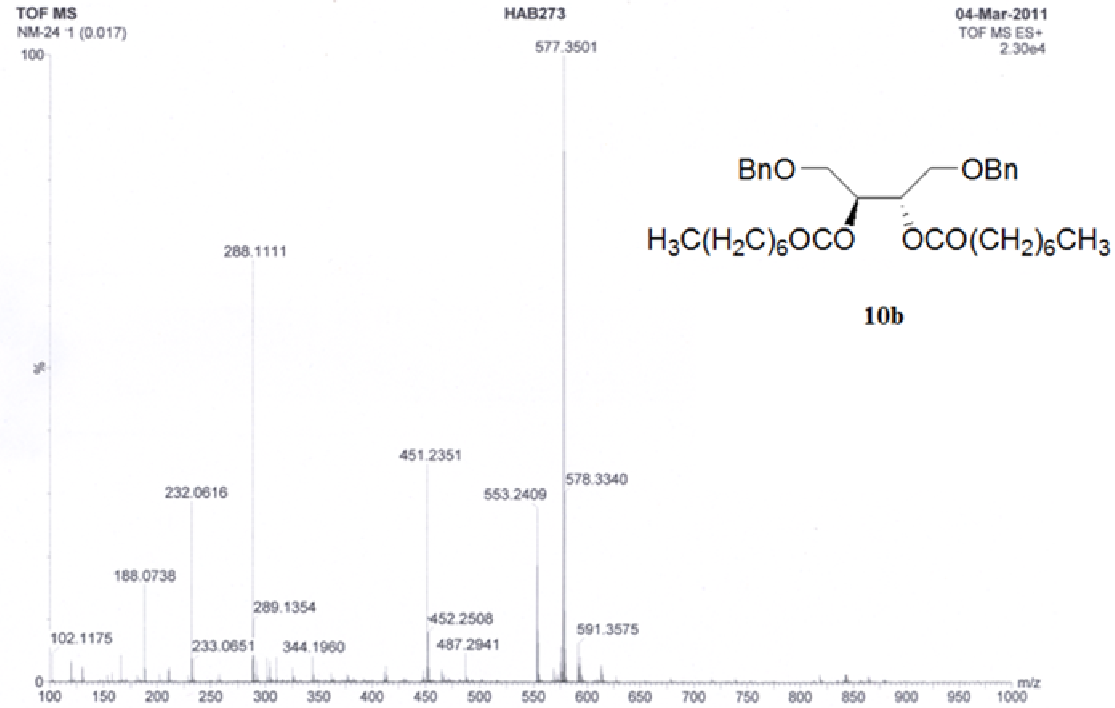

10b

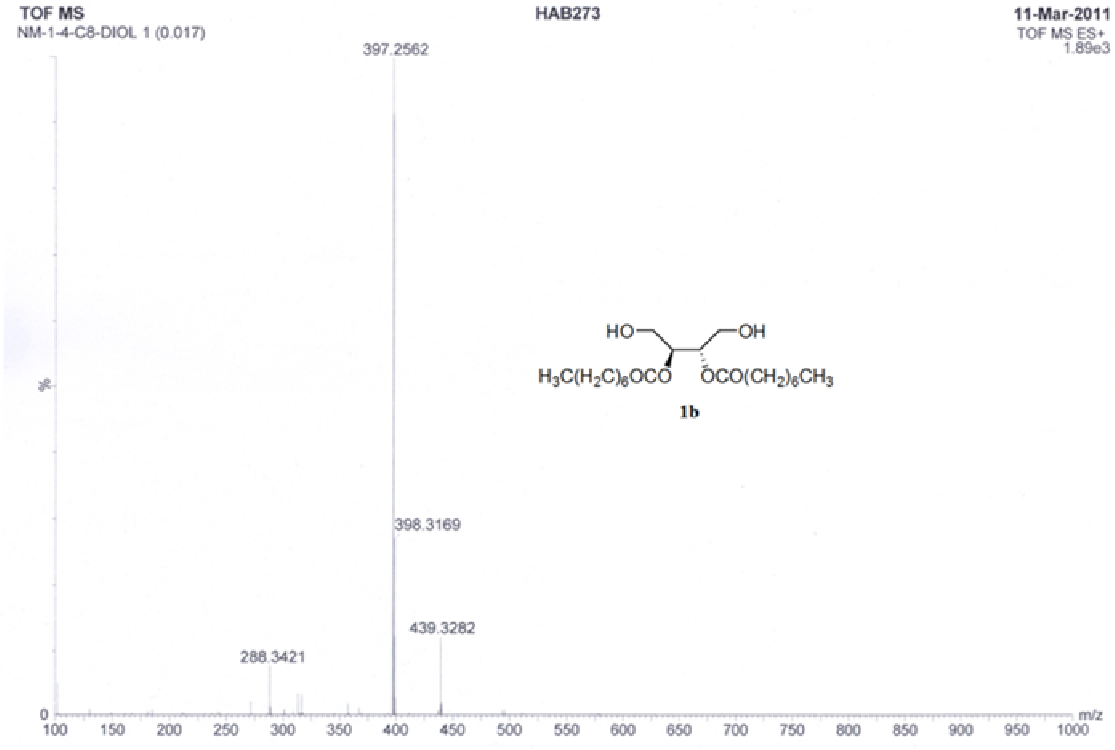
TOF MS
NM-1-4-C8-DIOL 1 (0.017)
HAB273
11-Mar-2011
TOF MS ES+
1.89e3
397.2562
398.3169
439.3282
288.3421
%
0
100 150 200 250 300 350 400 450 500 550 600 650 700 750 800 850 900 950 1000
m/z
HO
OH
H3C(H2C)6OCO
OCO(CH2)6CH3
1b

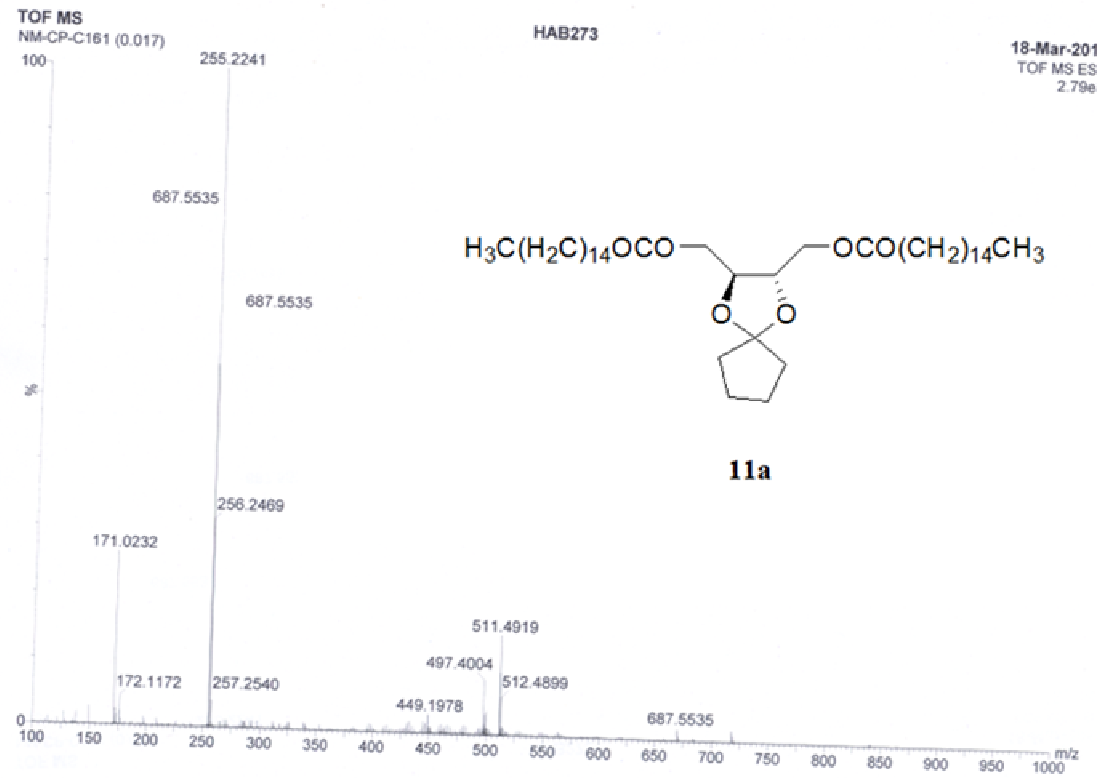
TOF MS
NM-CP-C161 (0.017)
HAB273
18-Mar-201
TOF MS ES
2.79e
100
255.2241
687.5535
687.5535
256.2469
171.0232
511.4919
497.4004
512.4899
172.1172
257.2540
449.1978
687.5535
%
0
100 150 200 250 300 350 400 450 500 550 600 650 700 750 800 850 900 950 1000
m/z
H3C(H2C)14OCO
OCO(CH2)14CH3
O
O
11a

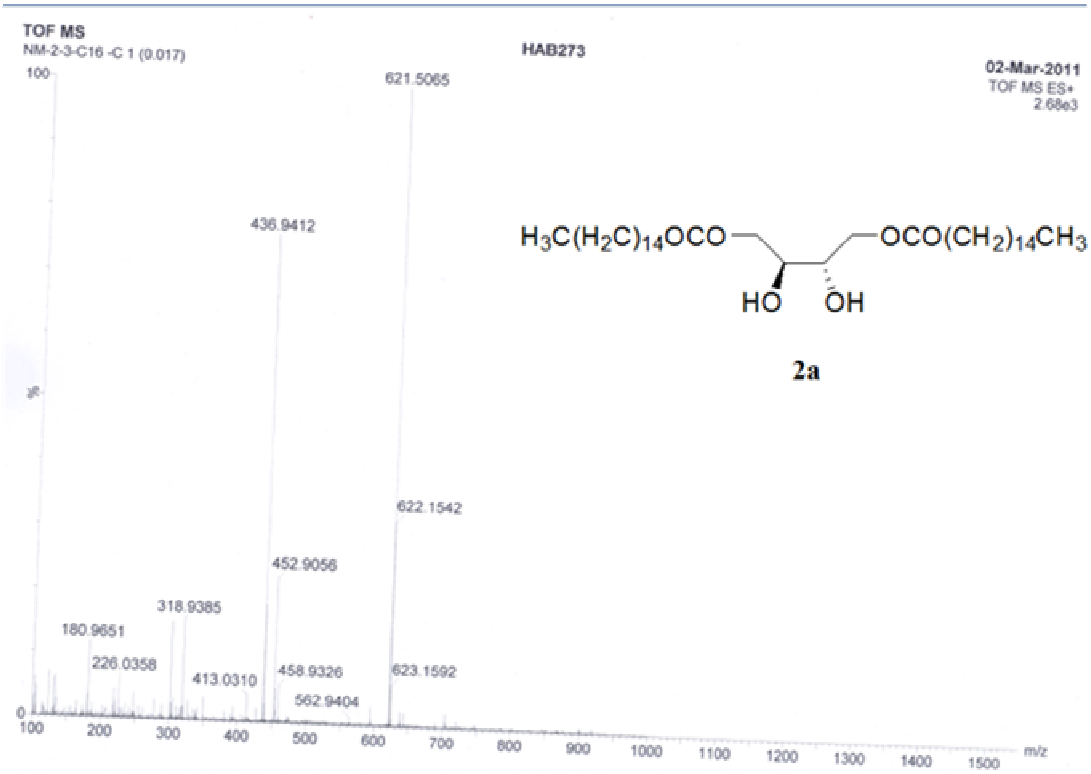

2a

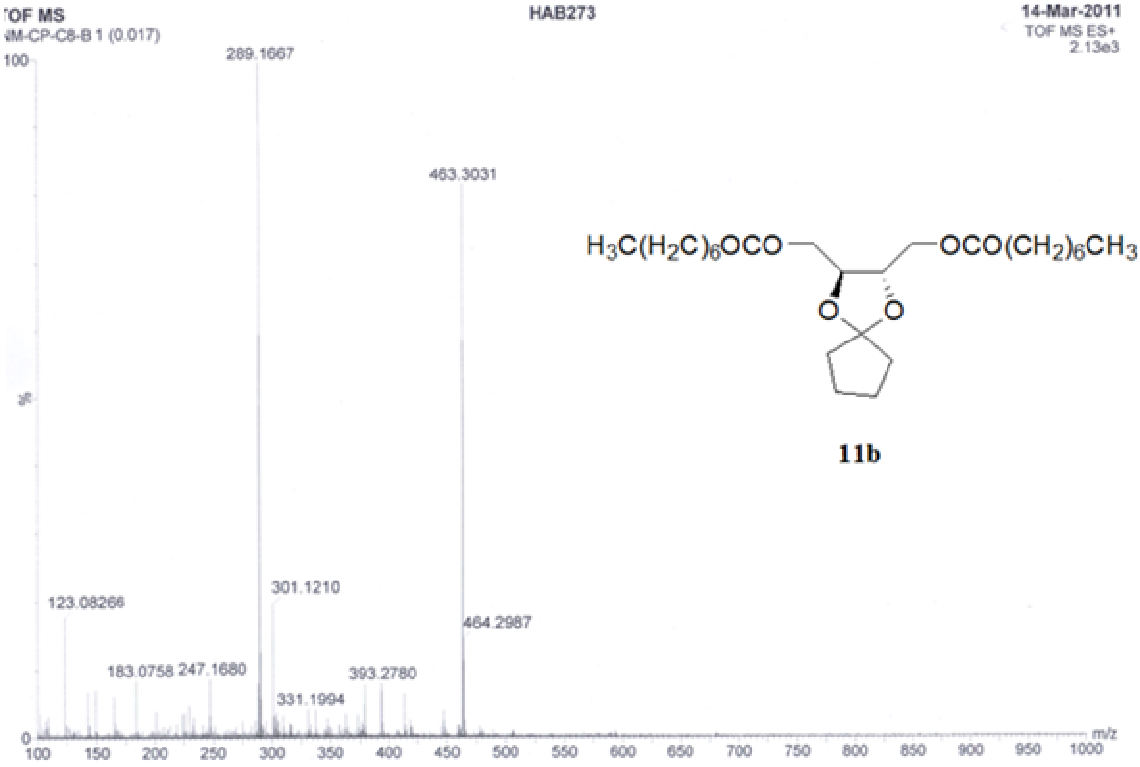

11b

Sample Name	DAT2B	Position	Vial 1	Instrument Name	Instrument 1	User Name	
Inj Vol	-1	InjPosition		SampleType	Sample	IRM Calibration Status	All Ions Missed
Data Filename	DAT2B.d	ACQ Method		Comment		Acquired Time	8/6/2011 4:01:46 PM

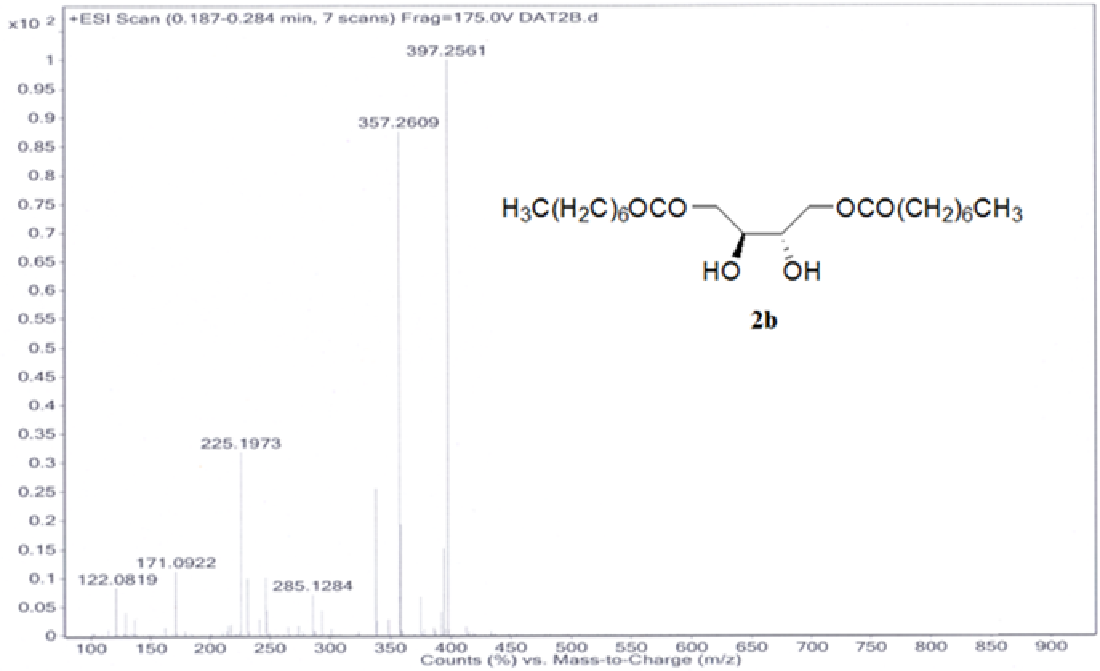

2b

Sample Name	NM_BN TARTRATE	Position	Vial 1	Instrument Name	Instrument 1	User Name	
Inj Vol	-1	InjPosition		SampleType	Sample	IRM Calibration Status	All Ions Missed
Data Filename	NM_BN TARTRATE.d	ACQ Method		Comment		Acquired Time	8/1/2011 6:53:22 PM

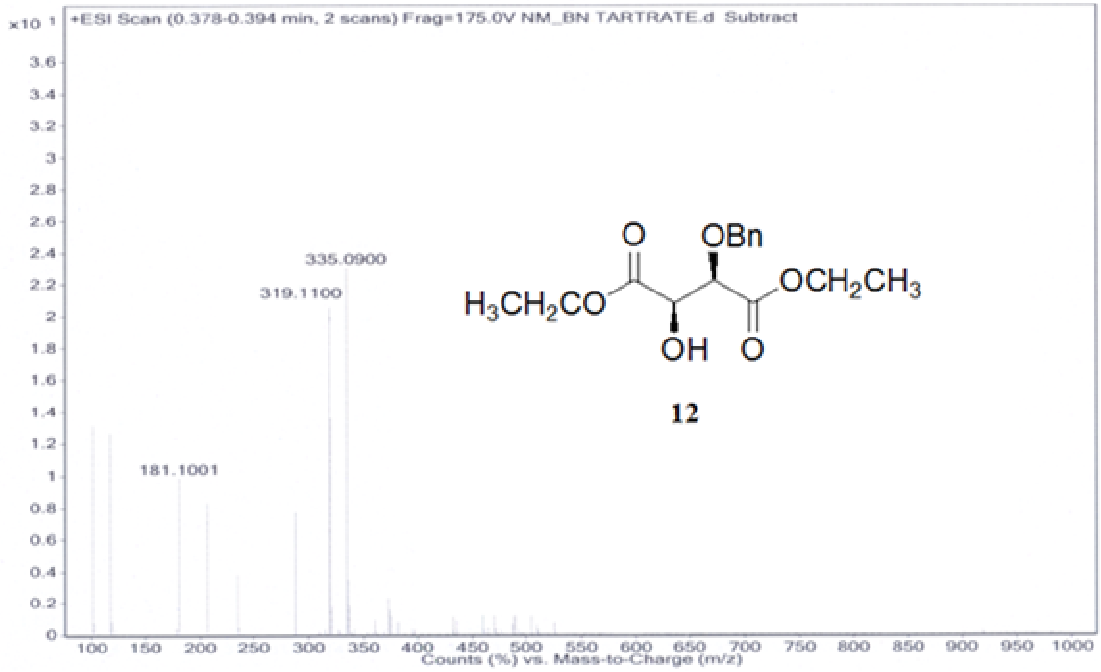

12

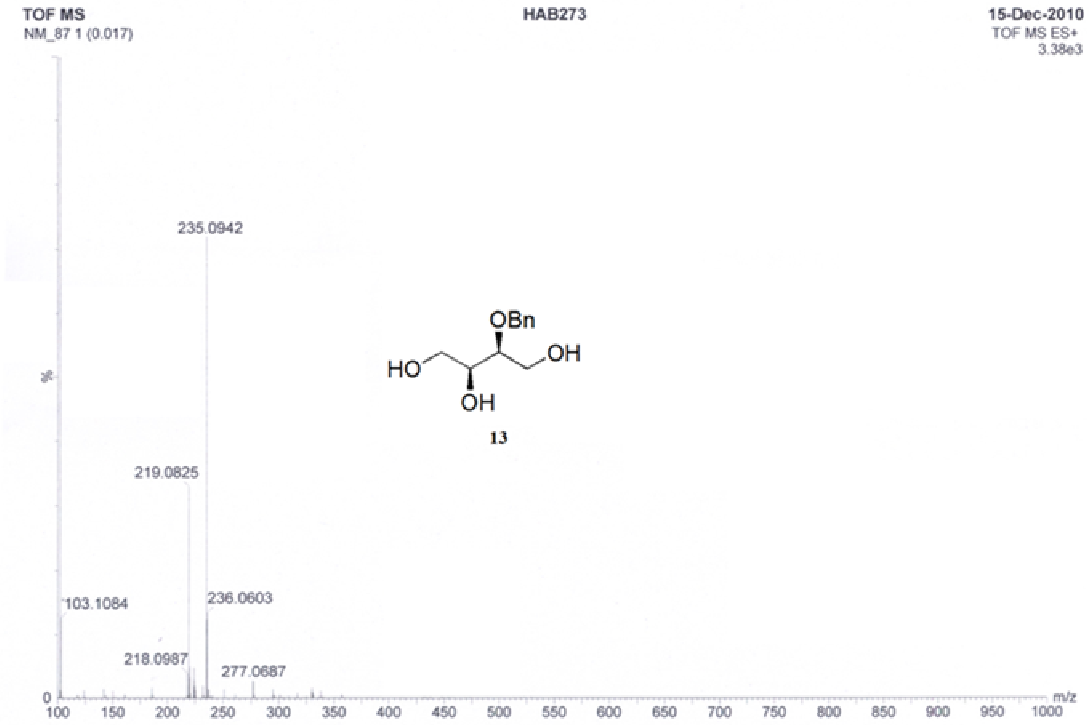

13

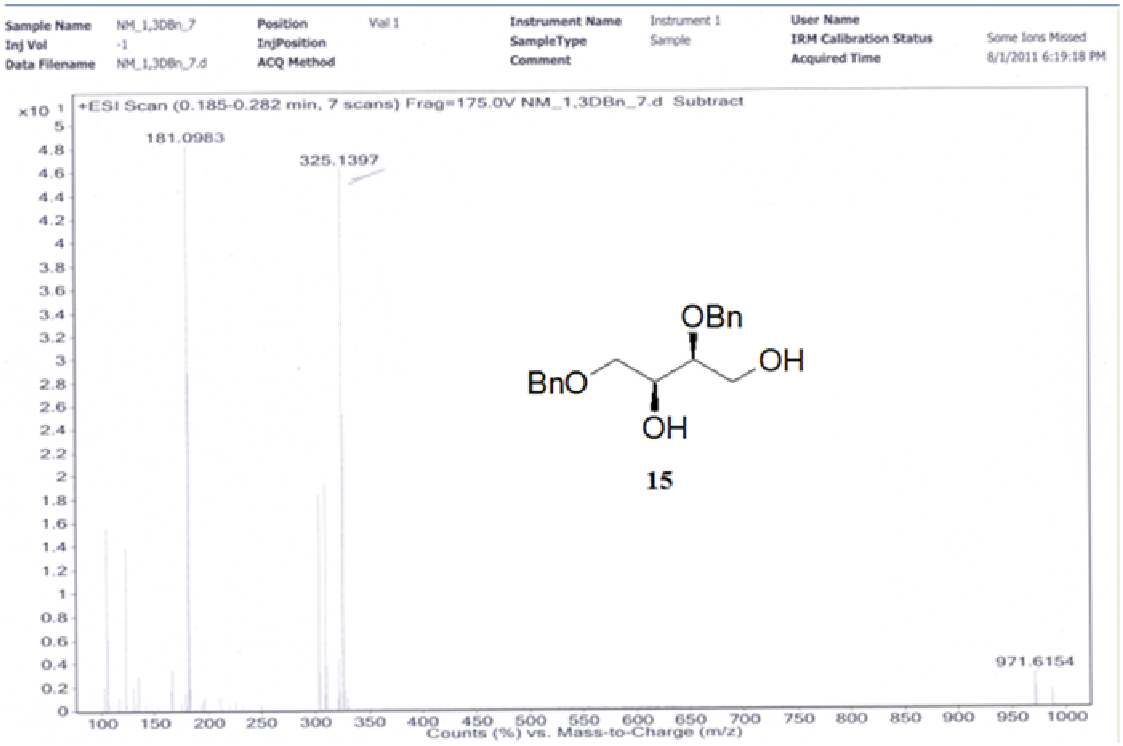

15

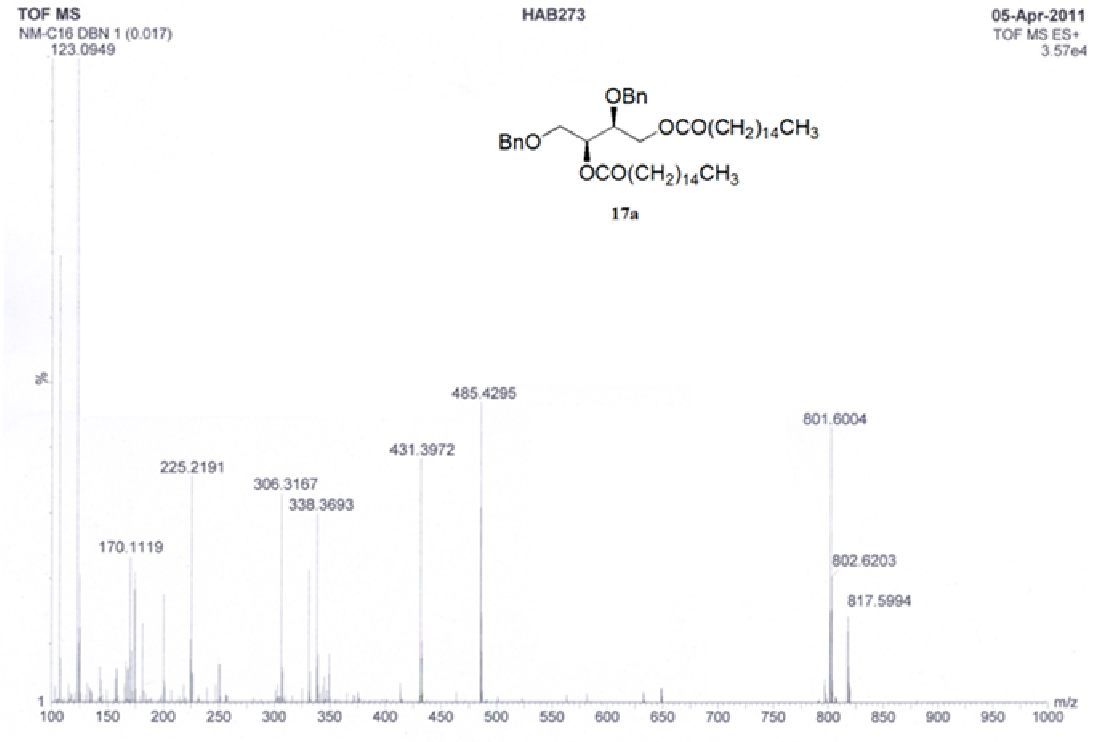
TOF MS
NM-C16 DBN 1 (0.017)
123.0949
HAB273
05-Apr-2011
TOF MS ES+
3.57e4
OBn
BnO
OCO(CH2)14CH3
OCO(CH2)14CH3
17a
%
485.4295
801.6004
431.3972
225.2191
306.3167
338.3693
170.1119
802.6203
817.5994
1
100 150 200 250 300 350 400 450 500 550 600 650 700 750 800 850 900 950 1000
m/z

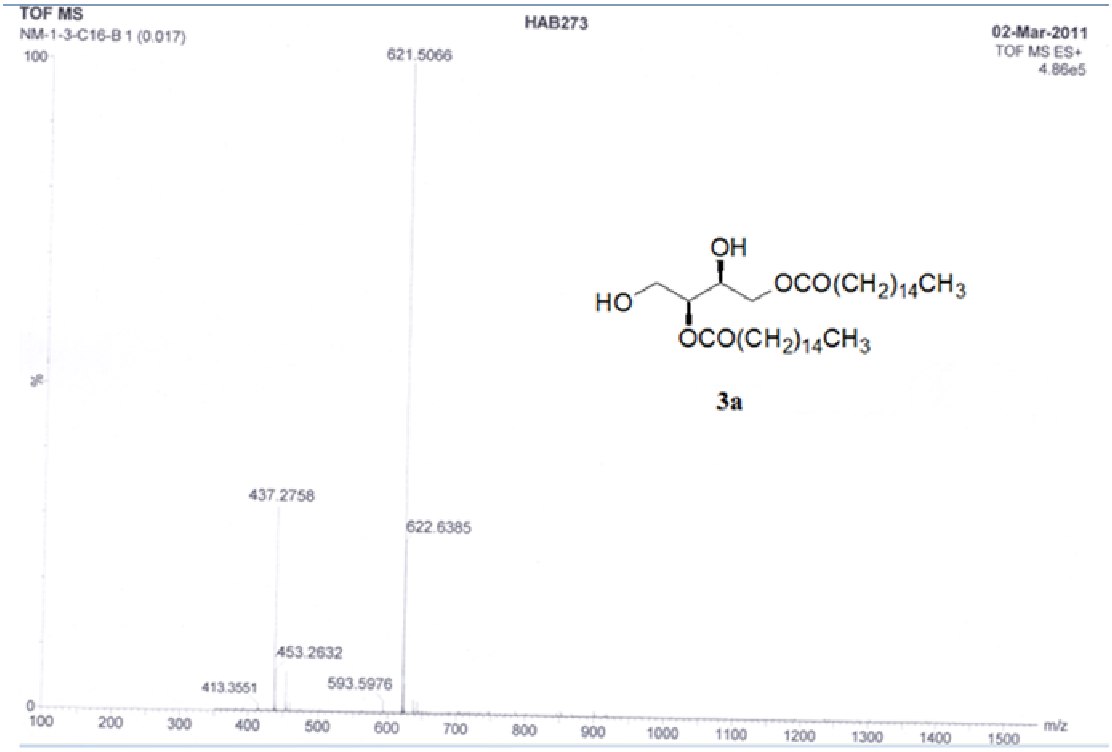
TOF MS
NM-1-3-C16-B 1 (0.017)
HAB273
02-Mar-2011
TOF MS ES+
4.86e5
100
621.5066
OH
HO
OCO(CH2)14CH3
OCO(CH2)14CH3
3a
%
437.2758
622.6385
453.2632
413.3551
593.5976
0
100 200 300 400 500 600 700 800 900 1000 1100 1200 1300 1400 1500
m/z

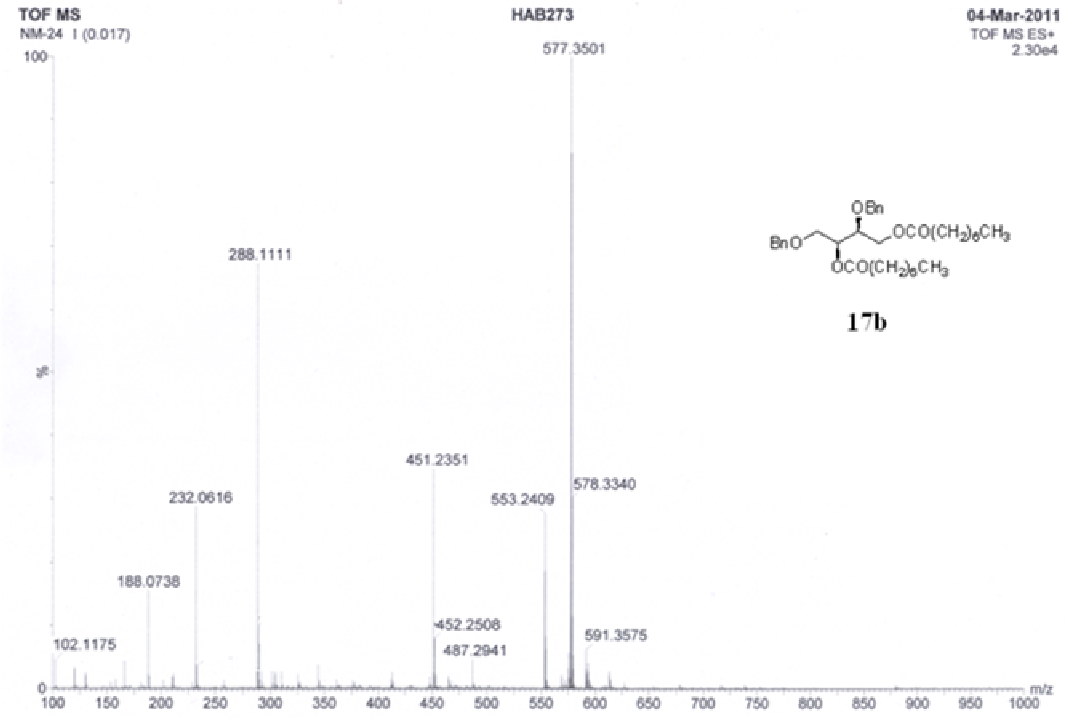

17b

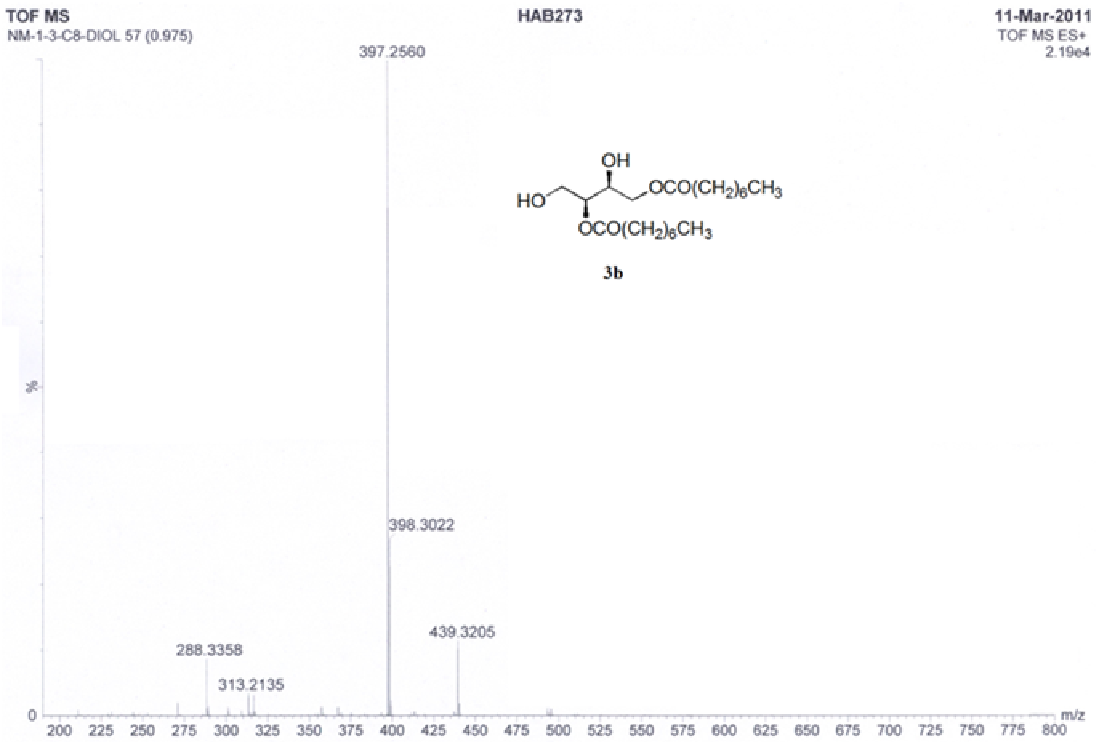

3b

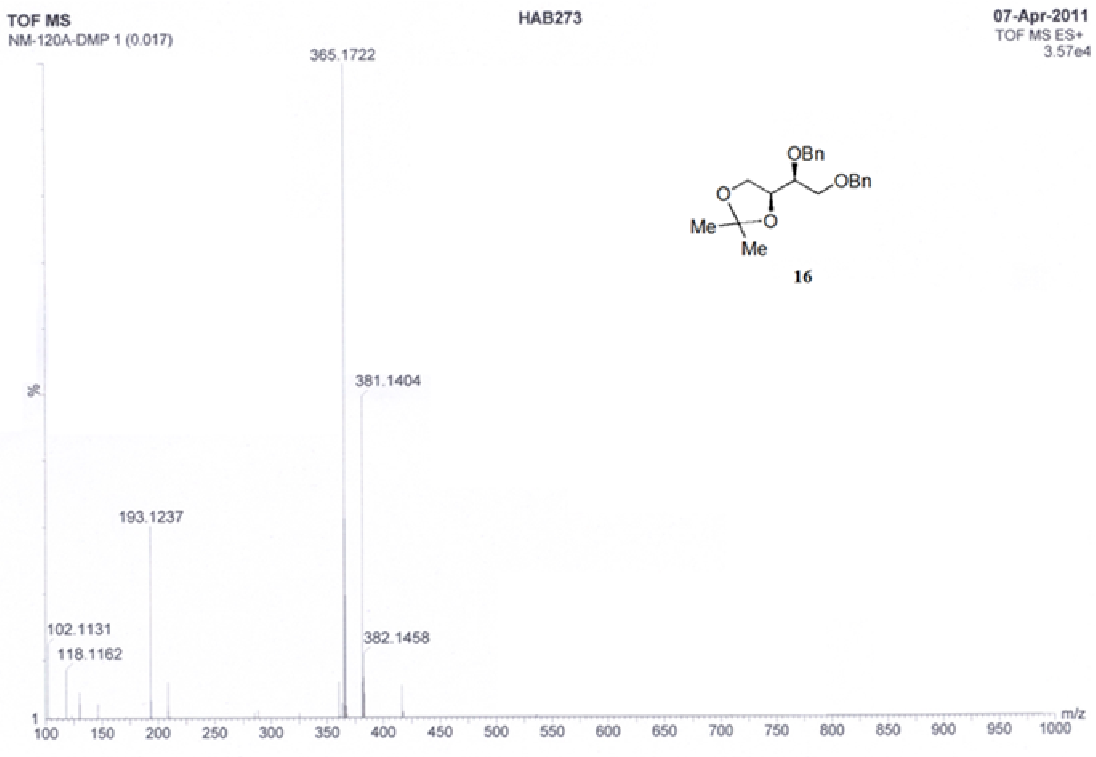

16

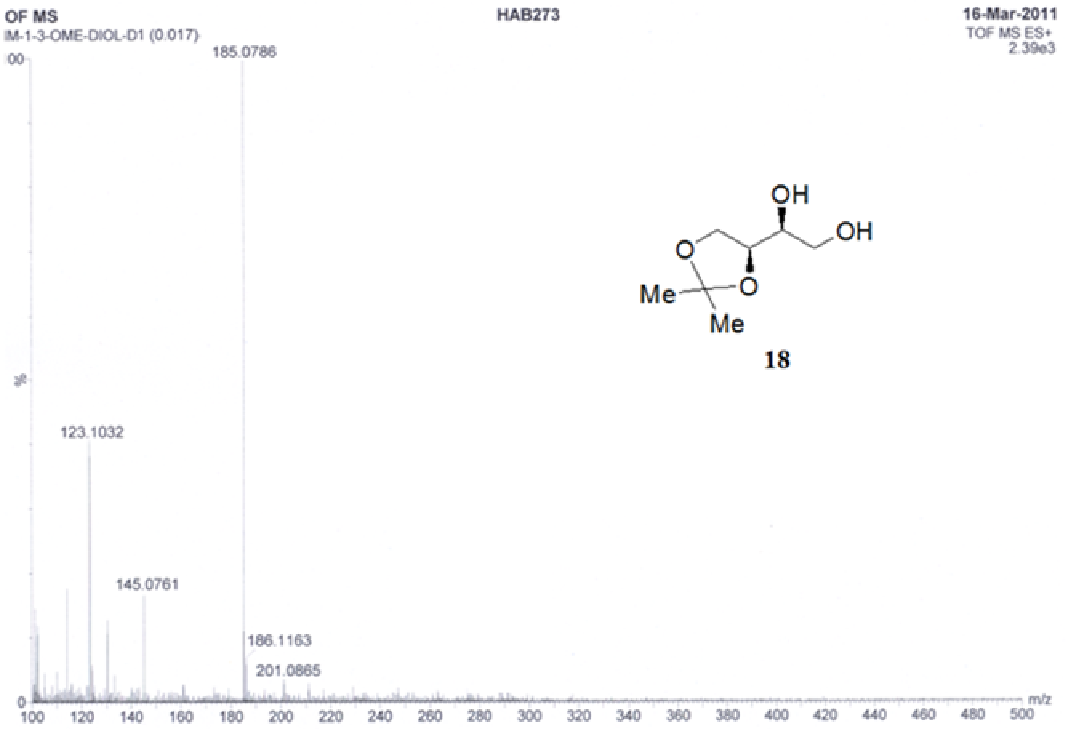

18

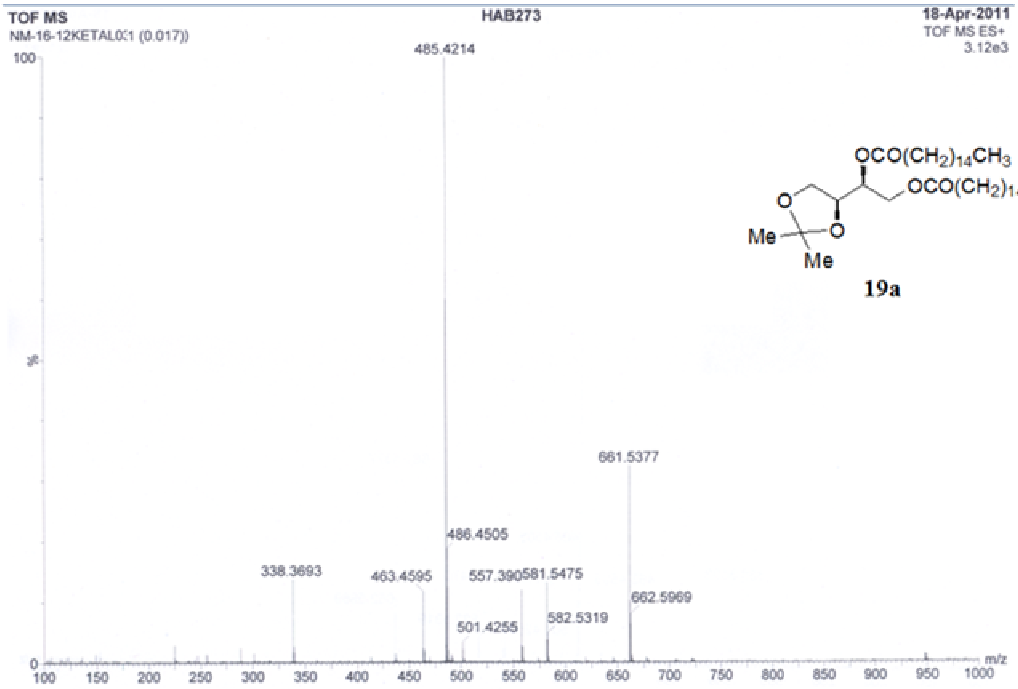
TOF MS
NM-16-12KETAL001 (0.017)
HAB273
18-Apr-2011
TOF MS ES+
3.12e3
485.4214
661.5377
486.4505
338.3693
463.4595
557.3905
581.5475
662.5969
501.4255
582.5319
OCO(CH2)14CH3
OCO(CH2)14CH3
O
O
Me
Me
19a
%
m/z

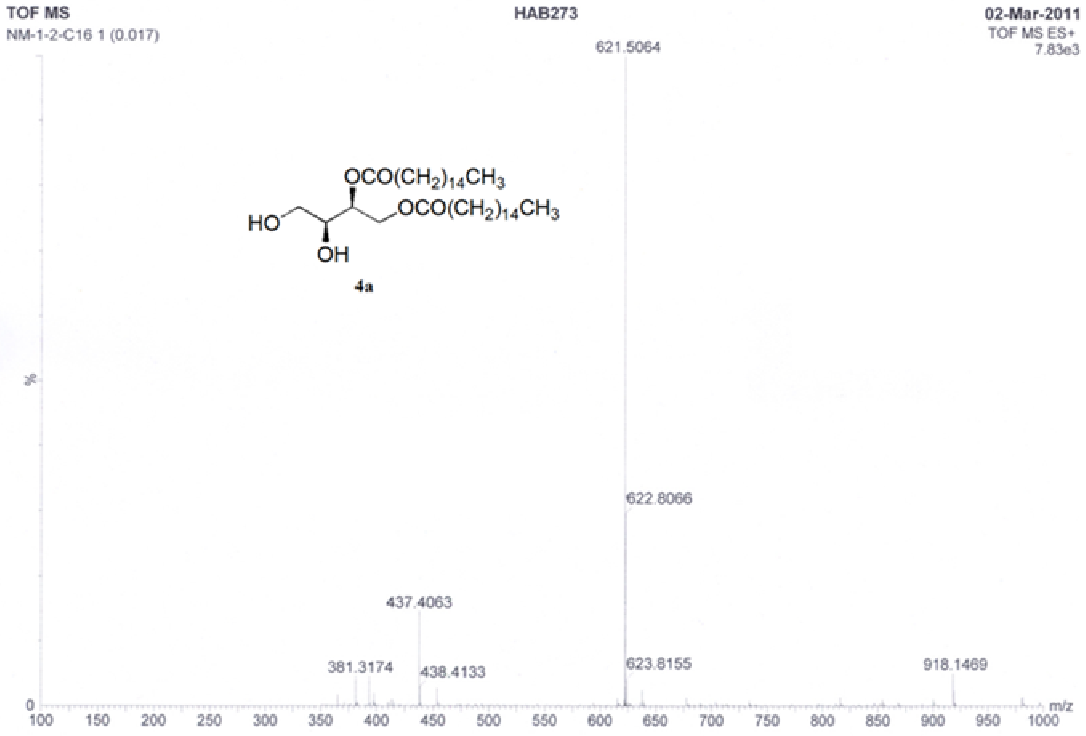
TOF MS
NM-1-2-C16 1 (0.017)
HAB273
02-Mar-2011
TOF MS ES+
7.83e3
621.5064
622.8066
437.4063
381.3174
438.4133
623.8155
918.1469
OCO(CH2)14CH3
OCO(CH2)14CH3
HO
OH
4a
%
m/z